UNIVERSIDADE D
COIMBRA

Armando Manuel Machado Remondes

CURCUMIN LOADED LACTOBIONIC ACID MODIFIED CHITOSAN-NANOPARTICLES FOR HEPATIC CANCER THERAPY

Dissertação no âmbito do Mestrado em Biologia Celular e Molecular orientada pela Professora Doutora Olga Maria Fernandes Borges Ribeiro e coorientada pela Professora Doutora Maria Paula Matos Marques Catarro e apresentada ao Departamento de Ciências da Vida da Faculdade de Ciências e Tecnologia da Universidade de Coimbra.

Julho de 2023

FACULDADE DE CIÊNCIAS E TECNOLOGIA
UNIVERSIDADE D COIMBRA

CURCUMIN LOADED LACTOBIONIC ACID MODIFIED CHITOSAN-NANOPARTICLES FOR HEPATIC CANCER THERAPY

Armando Manuel Machado Remondes

Candidature thesis for master's degree in Cellular and Molecular Biology, submitted to the Life Sciences Department, of the Faculty of Sciences and Technology of the University of Coimbra

Tese de candidatura ao grau de mestre em Biologia Celular e Molecular, apresentada ao Departamento de Ciências da Vida, da Faculdade de Ciências e Tecnologia da Universidade de Coimbra

Julho 2023

The experimental work presented in this thesis was developed under the scientific supervision of Professor Doctor Olga Maria Fernandes Borges Ribeiro, from the Pharmaceutical Technology Laboratory of Faculty of Pharmacy, University of Coimbra and co-supervision of Professor Doctor Maria Paula Matos Marques Catarro, from the Life Sciences Department.

This work was financed by the European Regional Development Fund (ERDF), through the COMPETE 2020 - Operational Programme for Competitiveness and Internationalisation and Portuguese national funds via FCT – Fundação para a Ciência e a Tecnologia, under project UIDB/04539/2020, UIDP/04539/2020 and LA/P/0058/2020

“Above all, don't lie to yourself. The man who lies to himself and listens to his own lie comes to a point that he cannot distinguish the truth within him, or around him, and so loses all respect for himself and for others.”

Fyodor Dostoyevsky

Agradecimentos / Acknowledgments

Gostaria de aproveitar este espaço para expressar o meu profundo agradecimento a todas as pessoas que foram fundamentais para a realização deste trabalho. Sem o contributo de cada um de vocês, esta jornada teria sido imensamente mais árdua.

Primeiramente, gostaria de agradecer à Professora Doutora Olga Borges, por me ter recebido no seu laboratório e pelo valioso acompanhamento e orientação ao longo de todo o processo. Os seus conselhos, esclarecimentos e dedicação foram decisivos no meu desempenho.

Aos alunos de doutoramento do "Nanolab", João e Mariana, o meu sincero agradecimento por tudo o que ensinaram, sem a vossa presença e ajuda o trabalho no laboratório teria sido infinitamente vezes mais difícil. Um agradecimento especial também aos meus colegas na batalha que é o mestrado, Alexandra e Paulo por toda a disponibilidade e paciência em me acompanharem atentamente ao longo do trabalho laboratorial. Além disto, um obrigado aos 4, por todos momentos de convívio compartilhados, que foram sem dúvida lufadas de ar fresco em dias longos.

Aos meus amigos de Mogadouro, à minha família, avós, tia, e especialmente aos meus pais, o meu profundo agradecimento por todo o apoio incondicional ao longo do meu percurso académico. Sem o vosso incentivo e amor, não teria sido possível chegar até aqui.

À família que construí em Bioquímica desde o primeiro dia da licenciatura - os "Amiguitos" - bem como a todos os meus descendentes. Às amizades que fiz durante o meu percurso associativista, desde a DG/AAC, à sua ARE até ao Conselho Geral da UC. Foram vocês que me proporcionaram momentos de escapatória e alívio depois de dias exaustivos, e, às vezes, infrutíferos.

À Íris. Se mantive a minha sanidade mental ao longo deste ano, é principalmente a ti a quem o devo. O meu mais profundo agradecimento por me teres emprestado a tua energia quando a minha era inexistente e por teres sido a minha mais forte e constante fonte de inspiração e felicidade.

Index

List of Figures

List of Tables

List of Abbreviations

ACK	Ammonium-Chloride-Potassium
Akt	Protein Kinase B
ASGPR	Asialoglycoprotein Receptor
Bcl-2	B-Cell Lymphoma
CAFs	Cancer-Associated Fibroblasts
CD44	Cluster Of Differentiation
ConA	Concanavalin A
COX-2	Cyclooxygenase-2
CS	Chitosan
CT	Computed Tomography
CTLs	Cytotoxic T Lymphocytes
DCFH-DA	Dichlorofluorescein Diacetate
DD	Deacetylation
DLS	Dynamic Light Scattering
DMEM	Dulbecco's Modified Eagle Medium
DMSO	Dimethyl Sulfoxide
DNA	Deoxyribonucleic Acid
ECM	Extracellular Matrix
EDC	1-Ethyl-3-(3-Dimethylaminopropyl) Carbodiimide
EGFR	Epidermal Growth Factor Receptor
ELISA	Enzyme-Linked Immunosorbent Assay
ELS	Electrophoretic Light Scattering
Erk	Extracellular Signal-Regulated Kinase
FBS	Fetal Bovine Serum
FDA	Food And Drug Administration
Gal	D-Galactose
GalNac	N-Acetyl-Galactosamine
GPCRs	G-Protein-Coupled Receptors
HBSS	Hank's Balanced Salt Solution
HBV	Hepatitis B Virus
HCC	Hepatocellular Carcinoma
HCV	Hepatitis C Virus

HEPES	4-(2-Hydroxyethyl) Piperazine-1-Ethanesulfonic Acid
HPCs	Hepatic Progenitor Cells
HSCs	Hepatic Stellate Cells
IFNs	Interferons
IL-1β	Interleukin-1 Beta
IL-6	Interleukin-6
iNOS	Inducible Nitric Oxide Synthase
IPST	Instituto Português Do Sangue E Da Transplantação
LA	Lactobionic Acid
LCSCs	Liver Cancer Stem Cells
LPS	Lipopolysaccharides
MAPK	Mitogen-Activated Protein Kinase
MRI	Magnetic Resonance Imaging
MTT	3-(4,5-Dimethylthiazol-2-Yl)-2,5-Diphenyltetrazolium Bromide
MW-CS	Medium Weight Chitosan
NAFLD	Nonalcoholic Fatty Liver Disease
NADPH	Nicotinamide Adenine Dinucleotide Phosphate
NF-kB	Nuclear Factor Kappa-Light-Chain-Enhancer of Activated B Cells
NHS	N-Hydroxysuccinimide
NPs	Nanoparticles
PBMCs	Peripheral Blood Mononuclear Cell
PBS	Phosphate-Buffered Saline
PHA-M	Phytohemagglutinin-M
PI3K	Phosphoinositide 3-Kinase
Raf	Rapidly Accelerated Fibrosarcoma
RANTES	Regulated Upon Activation, Normal T Cell Expressed and Secreted
Ras	Rat Sarcoma Virus
RBCs	Red Blood Cells
ROS	Reactive Oxygen Species
RPMI	Roswell Park Memorial Institute
SD	Standard Deviation
SEM	Standard Error of The Mean
STAT	Signal Transducer and Activator Of Transcription

TAM	Tumor-Associated Macrophages
TGF-β	Transforming Growth Factor Beta
TKRs	Tyrosine Kinase Receptors
TME	Tumor Microenvironment
TNF-α	Tumor Necrosis Factor Alpha
TPP	Tripolyphosphate
Tregs	Regulatory T Cells
VEGFR	Vascular Endothelial Growth Factor Receptor
YAP	Yes-Associated Protein

Abstract

Worldwide, hepatocellular carcinoma (HCC) is responsible for most liver cancer diagnoses and deaths. Primary liver cancer is the seventh most occurring type of cancer, and it is the fourth most responsible for mortal cases. In recent years, nanotechnology has been used as a tool for fighting HCC, mainly its early diagnosis and treatment of advanced forms, which has improved therapeutic agents aiming future clinical practices. Curcumin is a polyphenol which has been shown to target multiple signaling molecules, and proved to have antiangiogenic, anti-inflammatory, antioxidant, and antitumor effects, which applies to HCC. However, it has some limitations. Due to its hydrophobic characteristics result in poor solubility and absorption, rapid metabolism and elimination, necessitating the development of a safe delivery platform. Chitosan (CS), derived from a natural polysaccharide, the chitin, has been utilized for preparing nanoparticles and loading into them small pharmacologically active molecules. Chitosan has favorable properties such as good biodegradability, low toxicity, and easy modifiability. More recently, it has been discovered that CS itself possesses anti-carcinogenic and hepato-protective properties. The modifiability of this polymer is particularly advantageous as it allows to link some molecules for better targeting to specific cells. Specifically, by expressing galactose, CS can effectively target the Asialoglycoprotein Receptor (ASGPR) present on hepatocytes of human carcinoma cell lines. The objective of this work was to develop, characterize and study curcumin encapsulated lactobionic acid modified chitosan nanoparticles (NPs), which present a galactose moiety on chitosan's surface. These NPs were characterized for their cytotoxicity on hepatocellular carcinoma cells and healthy immune cells, registering overall no cytotoxicity at the tested concentrations. Additionally, their effect on oxidative stress was also verified, which confirmed curcumin's antioxidant potential. Their immune response profile was also studied, with none of the nanoparticles stimulating pro-inflammatory cytokines. These contributions could provide significant insights for future studies using these NPs, as a part of potential cancer therapy and immunomodulation.

Keywords: Curcumin; Chitosan nanoparticles; Asialoglycoprotein Receptor; Hepatocellular Carcinoma; Liver targeting

Resumo

O carcinoma hepatocelular (HCC) é mundialmente responsável pela maioria dos diagnósticos e óbitos de cancro do fígado. O cancro do fígado primário é o sétimo tipo mais frequente de cancro e o quarto mais mortal. Nos últimos anos, a nanotecnologia tem sido usada como ferramenta para o combater, especialmente no seu diagnóstico precoce e tratamento nas formas avançadas, o que tem melhorado os agentes terapêuticos com vista a futuras práticas clínicas. A curcumina é um polifenol que se tem demonstrado eficaz em interagir com várias moléculas de sinalização, possuindo efeitos antiangiogénicos, anti-inflamatórios, antioxidantes e antitumorais, que se aplicam ao HCC. Contudo, apresenta algumas limitações. Devido às suas características hidrofóbicas, a sua absorção é limitada, com metabolismo e eliminação rápidos, o que requer o desenvolvimento de uma plataforma de entrega segura. O quitosano (CS), um polissacarídeo natural, utilizado para carregar pequenas moléculas devido a possuir propriedades como boa biodegradabilidade, baixa toxicidade e fácil modificação. Mais recentemente, foi descoberto que o própria CS possui propriedades anti-cancerígenas e hepato-protetoras. Esta modificabilidade é particularmente vantajosa, permitindo um melhor direcionamento para células de HCC. Especificamente, ao expressar galactose na sua superfície, pode-se direcionar eficazmente para o recetor de Asialoglicoproteína (ASGPR) presente nos hepatócitos de células do HCC. O objetivo deste trabalho foi desenvolver, caracterizar e estudar nanopartículas (NPs) de quitosano modificadas com ácido lactobiónico e encapsulando curcumina, que apresentam uma unidade de galactose na sua superfície. Estas NPs foram caracterizadas quanto à sua citotoxicidade em células de carcinoma hepatocelular e células imunitárias saudáveis, não revelando toxicidade de um modo geral para as concentrações testadas. Adicionalmente, o seu efeito no stress oxidativo foi também verificado, onde se confirmou o potencial antioxidante da curcumina. O perfil imunológico também foi estudado, não se observando estimulação de citocinas pró-inflamatórias por parte das nanopartículas. Estas contribuições poderão fornecer detalhes interessantes para futuros estudos utilizando estas nanopartículas, tendo como objetivo potenciais terapias do cancro e estudos imunológicos.

Palavras-chave: Curcumina; Nanopartículas de Quitosano; Recetor de Asialoglicoproteína; Carcinoma Hepatocelular; Direcionado para o Fígado.

Chapter 1 - Introduction

1. Introduction

1.1 Hepatocellular Carcinoma

Hepatocellular Carcinoma (HCC) is a very aggressive type of primary liver cancer, which accounts for over 80 percent of all liver cancers, it is the seventh most common tumors disease and the fourth in terms of mortality associated with cancer, worldwide (Wen et al., 2022).

HCC can be originated by a wide variety of conditions, whether strictly cellular or environmental-related issues, but it mostly develops in people that already have liver problems (J. D. Yang et al., 2019). Most cases of HCC are derived from patients with hepatitis B virus (HBV) or hepatitis C virus (HCV). However, hepatitis does not pose as the single primary cause of HCC. High consumption of alcohol, which translates to cirrhosis and liver damage caused by inflammation and fibrosis; Moreover, other comorbidities like obesity and insulin resistance which can cause nonalcoholic fatty liver disease (NAFLD) are frequently associated with HCC diagnosis; Finally, smoking tobacco and the intake of food contaminants like the mycotoxin aflatoxin B1, all together are factors that in the long run can originate HCC. These causes are very geographic-dependent (J. D. Yang et al., 2019), for example, in the United States of America 35 percent of HCC cases were heavily linked to obesity and/or diabetes (J. D. Yang et al., 2019; Younossi et al., 2015), in Sub-Saharan countries like Sudan, 60 percent of HCC patients have a connection to aflatoxin B1 exposure (Magnussen & Parsi, 2013; Omer et al., 1998; J. D. Yang et al., 2019) and in the Asian continent, most cases are due to HCV or HBV infection and by high alcohol consumption (Ashtari et al., 2015; J. D. Yang et al., 2019). Understanding the multifaceted causes of HCC is crucial as it guides the selection of effective treatment approaches.

As we dwell into ways of treating HCC, it becomes evident that the management of this complex disease requires a comprehensive approach. The most common surgical interventions involve the removal of the liver or excerpts of the liver, with treatments like hepatic resection, liver transplantation and ablation techniques (Z. Chen et al., 2020). Chemotherapy plays an extremely limited role (Deng et al., 2015)

as a standalone therapy, with very modest results, limited response rates and overall survival benefits compared to other treatment approaches.

Nevertheless, these approaches are not as successful as desired, as reappearance of tumors are highly common on HCC, and they are hardly effective on fighting this phenomenon (Tsoulfas et al., 2014). In fact, only the resection and the transplantation of the liver are potentially curative treatments, although only 15% of patients are eligible for them and being only employed in the early stage of the disease (Crissien & Frenette, 2014).

Having this in mind, in recent years, novel therapies, targeting specific cells or pathways have been developed, particularly combining diverse types of therapies.

The first and standard FDA-approved drug for advanced HCC, which is considered a first-line treatment option, improving overall survival and being capable of delaying disease progression in clinical trials was sorafenib, a multikinase inhibitor. These inhibitors are important for HCC treatment due to their ability to target multiple signaling pathways involved in cancer progression, including angiogenesis, cell proliferation, and survival, decreasing tumor growth, and inducing cell death. Although providing just limited effectiveness due to the majority of patients not benefiting from sorafenib due to the genetic heterogeneity of HCC (Pang et al., 2022). Nowadays there are also other approved drugs for its treatment, namely other multikinase inhibitors, but also monoclonal antibodies (Psilopatis et al., 2023).

However, these two types of drugs possess downsides, such as side effects from different arrays, from immune-related adverse events to liver toxicity and gastrointestinal disturbances (Baldo, 2013). As stated earlier, cancer cells can also develop a resistance to these factors, leading to reduced treatment effectiveness (Pang et al., 2022). In the more technical part, they are expensive (Wagle & Spencer, 2021), and some could only be directed to a certain subgroup of patients, as stated before.

In recent studies, it has been proved that these and other effects can be reduced by natural compounds as they can act as radiosensitizers and chemosensitizers (Nisar et al., 2022), enhancing the sensitivity of cancer cells to radiation and chemotherapy respectively. These natural extracts can also play the role of biological protectors of

healthy tissues, with many of them having documented hepatoprotective activity (Madrigal-Santillán et al., 2014), as well as being able to alleviate treatment-related side effects (Q. Y. Zhang et al., 2018) while they develop a synergistic role together with conventional chemotherapy agents (Castañeda et al., 2022).

Nanotechnology offers a promising approach to reduce the toxicity of cancer treatment by specifically targeting cancer cells while sparing healthy cells. Using nanoparticles, drugs can be encapsulated and delivered directly to cancer cells, minimizing exposure to healthy tissues and reducing the systemic toxicity of the treatment. This targeted delivery approach allows for a more concentrated and effective action at the site of the tumor, while minimizing the adverse effects on healthy tissues. Furthermore, in addition to its therapeutic applications, nanotechnology has also contributed to the development of advanced diagnostic strategies for HCC. Techniques such as nano-CT, nano-MRI, and nano-fluorescence imaging offer highly sensitive and precise detection of HCC at the nanoscale. These diagnostic tools aid in early detection, accurate diagnosis, and monitoring of HCC, enabling timely intervention and improved patient outcomes (Xu et al., 2022).

These two approaches – the use of natural compounds and nanotechnology – have also been put together in recent years, with the co-delivery in nano formulations of both natural compounds and chemotherapeutic agents proving to decrease the chemotherapy dose, having a synergistic effect, as well as overcoming multidrug resistance (B. Li et al., 2022).

In summary, the integration of nanotechnology in HCC treatment provides a dual benefit. By enabling targeted drug delivery, nanotechnology reduces the toxicity of treatment by selectively delivering drugs to cancer cells. Additionally, advanced diagnostic technologies based on nanotechnology enhance early detection and monitoring of HCC. This combination of therapeutic and diagnostic strategies holds great promise for improving the effectiveness of HCC treatment (Xu et al., 2022).

1.1.1 The main actors

Hepatocytes are the main parenchymal liver cells, accounting for almost 80 percent of the liver mass, and have a long-life cycle (Holczbauer et al., 2022). They are involved in a series of activities, ranging from protein synthesis to detoxification, but

also playing a very important role in liver regeneration. Whenever this central ability is compromised, mainly due to these cells becoming senescent, the Hepatic Progenitor Cells (HPCs) are activated. Under normal conditions, HPCs are in a separate compartment, the Canals of Hering, which plays out to be an important location, due to the possibility of differentiating in hepatocytes or into cholangiocytes, which will be important in the regenerative process. (Holczbauer et al., 2022; Tummala et al., 2017)

In recent years, the tumor microenvironment (TME) has also been the target of some studies (Sevic et al., 2019), in particular the Hepatic Stellate Cells (HSCs) which, in normal conditions, store vitamin A and regulate sinusoidal circulation, but when activated by external factors form Cancer-Associated Fibroblasts (CAFs), which induce extracellular matrix (ECM) formation by synthesizing collagen and fibronectin (Barry et al., 2020) contributing to tumor proliferation.

The TME of HCC is also composed of immune cells, like peripheral blood mononuclear cells (lymphocytes and monocytes) and neutrophils. One of the most common characteristics of cancer is chronic inflammation evaluated throughout this type of cells. Tissue reprogramming is observed in many situations through the upregulation of growth factors and cytokines in the inflammatory microenvironment (Coussens et al., 2013). Different types of lymphocytes have showed different outcomes cancer growth: whereas cytotoxic T lymphocytes (CTLs) actually correlate with a positive prognostic (Zheng et al., 2021), regulatory T Cells (Tregs) in particular have immunosuppressive properties, playing a crucial role on the initiation of HCC carcinogenesis (H. Wang et al., 2021). Monocytes infiltrate the tumor tissue and differentiate into tumor-associated macrophages (TAM) (Arvanitakis et al., 2022). They can display the M1 or M2 phenotypes, depending on the surrounding microenvironment: the M1 macrophages being associated with good prospects in cancer fight, whereas the M2 support angiogenesis and express immunosuppressive receptors (Jayasingam et al., 2019). Neutrophils can also display both anti and protumorigenic phenotypes (the so called N1 and N2 phenotypes, respectively), with this differentiation depending on the surrounding stimuli as well. For example, if there is a high concentration of TGF-β they will follow the protumoural route and favor angiogenesis, tumor growth and

immunosuppression. With a blockade of TGF-β or the presence of type I interferons (IFNs) they will drive towards an antitumoural path with a more immunostimulatory profile (Fridlender et al., 2009). The spleen also contributes to the continuous proliferation of immune cells in the TME, by being a reservoir of neutrophils and monocytes that can be mobilized in response to inflammation and later turn into M2 TAM or N2 neutrophils(Cortez-Retamozo et al., 2012; Jiang et al., 2021). Not only this, but there have been reports that these tumor associated neutrophils can in fact infiltrate tumor tissue in response to sorafenib treatment, recruiting macrophages and subsets of lymphocytes (Treg cells) in order to promote sorafenib resistance and enhancing HCC growth (S. L. Zhou et al., 2016).

Still regarding the influence of the immune and pro-inflammatory response in the development of HCC, there are also several reports which can correlate them to its evolution through various pathways. Interleukin-6 (IL-6) is one of the most extensively studied pro-tumorigenic cytokines being even classified as a lynchpin between inflammation and cancer. In recent years, it has been studied precisely due to being a possible target to control tumor growth. As mentioned earlier, macrophages in a cancer-related scenario, can undergo differentiation into M1 or M2 macrophages, being the first ones anti and the second ones pro-tumorigenesis. There are studies that relate the inhibition of IL6/STAT3 pathway to a better prognostic of cancer development, as with the blockage of this pathway, there is a significant increment on M1 differentiation, and consequent suppression of cell invasion, metastasis formation and an increase on malignant cells' apoptosis (L. Chen et al., 2018). TNF-α also plays a critical role in immune regulation. While it is essential for maintaining a balanced immune system, excessive or inappropriate production of TNF-α can have detrimental effects and contribute to the development of various diseases. On this line of thought, it has been documented as serving as a key connecting inflammation and the formation of tumors, and, in the specific case of HCC, to promote sorafenib-resistance (Tan et al., 2019). There are also reports suggesting that the inhibition of TNF-α can repress the formation of hepatocellular carcinoma associated cell metastasis, through downregulation of the Erk1/2 pathway (Y. H. Zhang et al., 2015).

Liver Cancer Stem Cells (LCSCs) have intermediate characteristics of HPCs and mature hepatocytes, which has led to studies regarding to their origin, which have concluded that these types of cells can reprogram themselves and dedifferentiate into LCSCs, when facing liver injury conditions. These cells, have somewhat known roles in tumor initiation and growth, on the processes of metastization and recurrence and provide the means for resisting therapy, however these mechanisms are not fully understood (Nuozhou Wang et al., 2018).

1.1.2 Cell surface proteins on HCC

Cell surface proteins play crucial roles in various cellular processes, including cell communication, adhesion, recognition, and signaling. Through these proteins the cell interact with other types of cells and compounds present on the extracellular environment. Siracusano et al., 2020 performed a comprehensive multi-omics analysis to characterize the molecular profiles of HCC tissues, with a particular focus on the cell surface proteome. This approach provided valuable insights into the changes in protein expression and their implications in HCC progression. Similarly, other researchers such as da Fonseca et al., 2020; Peng et al., 2018; Shi et al., 2013; Zhang et al., 2021 have also explored the cell surface proteome in HCC. This allowed for an extensive comprehension of HCC markers, ranging from receptors, cell adhesion molecules, transporters, and other cell surface associated proteins, which has proved to be helpful in the development of new therapies.

1.1.2.1 Membrane Receptors

Tyrosine Kinase Receptors (TKRs) serve as key players in cell proliferation, due to their abundance and significant influence on growth factor signaling within the receptor family. The most common type of receptors are the Epidermal Growth Factor Receptor (EGFR), expressed on 68% of HCC tissues and the Vascular Endothelial Growth Factor Receptor (VEGFR) which is deeply important in vascularization and angiogenesis (Mathonnet et al., 2006). When TKRs are activated through the binding of specific molecules, such as growth factors, cytokines, or hormones, a cascade of cellular events is triggered. Epidermal growth factor (EGF) is a well-known ligand that binds to and activates TKRs, leading to the upregulation of tumor cell proliferation, antiapoptotic effects, angiogenesis, and metastasis (da Fonseca et al., 2020; Huynh et al., 2012). This effect is mostly due to an activation of

certain pathways such as Ras-Raf-MEK-ERK (Y.-J. Guo et al., 2020), PI3K/Akt (Sun et al., 2021) and the protein kinase C pathway (K. Guo et al., 2008). Certain pharmaceuticals have been studied to precisely inhibit this activation of TKRs, and Sorafenib is an example of a dual-action Raf kinase and VEGFR inhibition preventing tumor cell proliferation and angiogenesis (S. Kim & Abou-Alfa, 2014), however it has limited efficacy mostly due to its side effects, that can go from gastrointestinal problems to hypertension (Zhu et al., 2017). It is important to note that the VEGF receptor pathway and Raf kinase are critical for the normal physiological function and homeostasis of various organs. Blocking these signaling pathways with Sorafenib can lead to therapeutic benefits by inhibiting tumor growth, but it can also result in significant toxicity profiles, hence these side effects (Ye Li et al., 2015).

G-Protein-Coupled Receptors (GPCRs) have been stated as having an important role on metastization and HCC progression, by modulating diverse pathways, however the mechanisms surrounding this are not yet clear (Peng et al., 2018). It is known that pathways such as those involving Wingless-related integration site (Wnt), Notch, Transforming Growth Factor Beta (TGF-β), as well as Phosphoinositide 3-kinase (PI3K) and Mitogen-activated protein kinase (MAPK) downstream kinases are triggered by these types of receptors. Dysregulations at the Wnt/β-catenin pathway lead to several cellular processes with consequences on the HCC proliferation (initiation, growth, survival, motility, differentiation, and apoptosis) (Khalaf et al., 2018). The Notch pathway is heavily associated with, metastasis formation and with the tumor microenvironment (TME) regulation, being involved in the recurrence of cancer stem cells (CSCs) (Huang et al., 2019). TGF-β signaling is implied throughout all stages of cancer injury, from the initial fibrosis formation to the development of HCC (Jin et al., 2022). Chemokine Receptors, Adrenergic Receptors, and Estrogen Receptors represent the predominant classes of GPCRs, with extensive research focusing on their clinical implications and potential therapeutic interventions (Peng et al., 2018). However, these interventions have some limitations, namely problems in their ligand identification (Usman et al., 2020).

The Cluster of Differentiation 44 (CD44), is a hyaluronic acid receptor, and interacts with ligands from the extracellular matrix (ECM), mediating cell adhesion and

migration (Z. Yang et al., 2018). It is highly expressed at first contact between carcinogen agents and hepatocytes, and it has been shown to downregulate the expression of p53, by activation of the Akt pathway, which will reduce programmed cell death, and allow for the perpetuation of the mutations associated with the tumorigenesis present on the cells (Dhar et al., 2018). It will also upregulates the expression of Yes-Associated Protein (YAP), which will allow a quick activation of oncogenes (Zhang et al., 2018). There have been some studies showing that high cholesterol levels are capable of inhibiting metastasis formation by regulating immune function, by sequestrating CD44 into lipid rafts (Z. Yang et al., 2018). However, it is noteworthy that excessive cholesterol levels can also activate mechanisms that promote tumorigenesis (Zhou & Sun, 2021), so this form of treatment has not proven to be a viable option due to these conflicting effects.

Asialoglycoprotein Receptor (ASGPR) is a lectin expressed on the surface of hepatocytes. These receptors are responsible for the binding, endocytosis, and degradation of extracellular glycoproteins with exposed, non-reducing terminal D-galactose (Gal), lactose or N-acetyl-galactosamine (GalNac) residues (Shi et al., 2013). They have the particularity of being a highly expressed protein on the membrane of hepatocytes and barely existing on other cells (D'Souza & Devarajan, 2015), with their expression levels increasing under cirrhotic conditions (Roggenbuck et al., 2012). Remarkably, these receptors have been found to resist degradation within lysosomes upon internalization of their ligand molecules, and returning to the membrane (Tanabe et al., 1979), further highlighting their potential as promising targets for active delivery strategies. During the last decade, these characteristics inherent to ASPGRs have made them subject of various studies that have as objective the active delivery of bioactive compounds to them (Alonso, 2018) which have allowed for different positive outcomes, like enhanced adhesion, delivery, functionality and higher efficacy and viability, with no toxicity. Clinical trials have yet to provide a more profound understanding of these formulations.

These cell surface proteins, act as key mediators of cell communication and signaling, intricately regulating vital cellular processes, and holding significant implications for the development of novel therapies. By modulating the interactions between cells and their environment, these proteins offer valuable insights into the

complex mechanisms underlying disease progression, including HCC, presenting promising avenues for therapeutic interventions.

1.2. Curcumin - an antitumor compound

In recent years, there has been a revival of interest in studying the usage and effectiveness of medicinal herbs to treat various diseases. Curcumin is an essential ingredient of turmeric plants, such as *curcuma longa*, commonly known as saffron. Geographically, *curcuma longa* is endemic in Southeast Asia, and has been present in traditional medicine from this part of the globe for centuries. The molecular formula of curcumin is $C_{21}H_{20}O_6$.

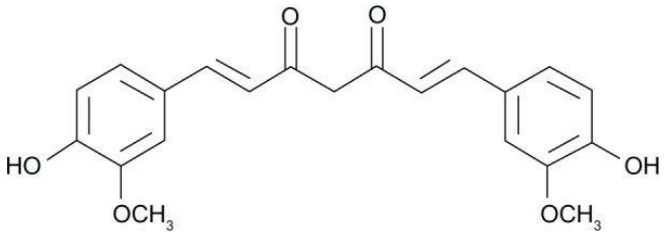

Figure 1. *Chemical structure of curcumin.*

This compound has been studied due to its antioxidant, anti-inflammatory and anti-cancer properties, which may help fighting against various diseases, such as cancer (Mansouri et al., 2020) and some neurodegenerative diseases (S. Hu et al., 2015). Its therapeutic characteristics have been widely exploited, and some of the proper mechanisms that allow us to consider curcumin as a promising therapy have already been described.

The curcumin is a polyphenol (Figure 1) with antioxidant activity (Chen et al., 2020), which has been further analyzed with studies proving the increased activity of antioxidant enzymes by curcumin (X. Lin et al., 2019), and the attenuation of lipid peroxidation (Nisari et al., 2017).

Regarding the anti-inflammatory property, a study (Kocaadam, 2017) has showed curcumin to be capable of inhibiting NF-kB activation. According to Camacho-Barquero et al., 2007, there is evidence suggesting reduced expression of enzymes such as inducible nitric oxide synthase (iNOS) and cyclooxygenase-2 (COX-2), which is associated with a decrease in NF-kB activity. The curcumin can also suppress Janus kinase-STAT inflammatory signaling, which will lead to an downregulation of the expression of inflammatory cytokines. This decrease on the production of the

pro-inflammatory cytokines, including TNF-α, IL-6, and IL-1β, was documented by G.-Y. Kim et al., 2005.

Moreover, there are studies that show that curcumin have the capacity of inducing apoptosis, which will then prevent tumor growth and also the suppression of cell cycle, regarding human lung, breast, prostate, colorectal, liver, carcinoma, pancreatic, myeloma, and melanoma cancers (Karthikeyan et al., 2020). There is also a study (Binion et al., 2008) that takes into account the antiangiogenic capacity of curcumin by inhibiting VEGF. For cancer proliferation in general, cell migration and invasion is an important factor, which is even more highlighted in HCC, as the recurrence poses as one of the major obstacles for treatments, so it has also been observed (Naizhi Wang et al., 2020) that curcumin can in fact inhibit these events on small lung cancer cells.

Apart from these therapeutical effects, curcumin has another positive characteristic, that is its safety profile, with little to no toxicity, and not displaying any mutagenic effects or other pathological effects, even in high dosages (Chainani-Wu, 2004). Nevertheless, it is far from being perfect as it has poor pharmacokinetics. One consequence of this is that when we ingest food rich in curcumin, it doesn't translate into a higher uptake of curcumin, as it is easily and rapidly metabolized and consequently excreted, leading to a poor absorption and bioavailability, highly due to its hydrophobic profile (Cas & Ghidoni, 2019).

Consequently, one of the primary research goals entails surmounting the aforementioned impediment and elucidating methodologies aimed at increasing curcumin bioavailability. One hypothesis could be by directly conjugating curcumin with other components to increase the solubility. Additionally, the desired outcome is for curcumin to reach its intended target tissue, thereby facilitating the exertion of its anticancer properties. This objective can be attained through the encapsulation within delivery systems such as nanoemulsions, lipid, polymer, and gel nanoparticles with the possibility. These encapsulation techniques, among other characteristics afford an extended period of circulation in the body, fostering prolonged contact with target cells and thereby enhancing the efficacy of its anticarcinogenic activity.

1.3. Chitosan and Chitosan Nanoparticles

Chitosan (CS) is a cationic polymer, consisting of glucosamine and N-acetylglucosamine units (Figure 2), derived through partial deacetylation of the chitin. The chitin is the second most abundant polysaccharide, following cellulose and is present on the exoskeleton of various species of crustaceans and insects. The term "chitosan" is used to refer to a wide array of similar polymers, whose differences are the degree of deacetylation (DD) and molecular weight. The DD is the ratio of glucosamine to N-acetylglucosamine units, and differences on it highly influence physicochemical behavior and biological functionality of the polymer (Szymańska & Winnicka, 2015).

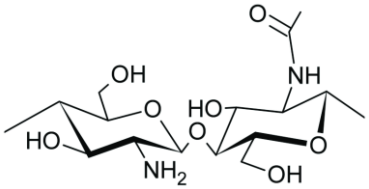

Figure 2. *Chemical structure of chitosan.*

Chitosan has been widely used on formulation of nanoparticles for targeted delivery, because it has favorable characteristics such as nontoxicity, biodegradability and biocompatibility, combined with very strong mucoadhesive properties, due to its positive charge which enables it to efficiently attach to cells, increasing the probability of cellular uptake (Garg et al., 2019). Chitosan also displays a very good stability and shelf life, which allows it to be stored over relatively long periods of time (Morris et al., 2011). This is important for the industry, particularly for logistic and technical questions, such as transportation and storage in facilities with lower budgets, for example, at countries with underdeveloped health care politics and conditions. It has also been reported (Jhaveri et al., 2021) that this polymer can be somewhat easily modified and functionalized, which opened the possibility to express certain molecules on the surface of the nanoparticles prepared with chitosan.

Together with these factors that make it already a valuable nanocarrier, chitosan nanoparticles have been documented has having the capability of opening tight junctions (Vllasaliu et al., 2010; Jian Zhang et al., 2014), a capacity that has been associated with the activation of the Protein Kinase C pathway (Vllasaliu et al., 2010), enhancing macromolecular permeability across epithelial cell lines and

overcoming an obstacle regarding bioavailability of the compounds encapsulated into chitosan particles in addition to enabling the molecular stability through the gastrointestinal tract.

Lastly, there have been extensive reports (Sharan Adhikari & Nath Yadav, 2018) on the last decades suggesting and explaining chitosan's direct therapeutic effects, meaning that chitosan on its own possesses characteristics that can make it a candidate for possible therapies. It possesses an hepatoprotective effect (Mohamed Zedan et al., 2021), as it is capable of displaying antioxidant mechanisms (Abd El-Hack et al., 2020; Mo et al., 2022). There are also reports that claim chitosan's antiangiogenic potential on HCC (Xu et al., 2009) , and its' capability of inducing apoptosis by caspase activation and arrest of cell cycle in oral (Wimardhani et al., 2014) and bladder (Hasegawa et al., 2001) cancer cells, as well as its antimicrobial activity (Abd El-Hack et al., 2020). Not only this, but chitosan has long been reported has having the potential to enhance immune response, by stimulating cells of the immune system (Zaharoff et al., 2007) as well as to reduce inflammation (Mohyuddin et al., 2021).

1.3.1 Chitosan Nanoparticles on Curcumin delivery

To overcome curcumin's previously mentioned major obstacles of poor water-solubility and subsequently low bioavailability, there have been several approaches, and one of these possibilities is the encapsulation of the curcumin into chitosan nanoparticles using different methods reviewed by Q. Hu & Luo, 2021. Pharmacokinetic and dynamic properties of several formulations regarding curcumin encapsulation into chitosan were discussed at Saheb et al., 2019.

Other researchers like Lopes et al., 2021 proved that there was in fact an improvement of both *in vitro* and *in vivo* effects of the encapsulated curcumin, and other studies have further proved that chitosan nanoparticles loaded with curcumin do provide antitumor activity on breast (Abdel-Hakeem et al., 2021), pancreatic (Arya et al., 2018), oral (Mazzarino et al., 2015) and cervical (Khan et al., 2016) cancer cells. On these studies it was observed the antiproliferative capacity of the curcumin loaded chitosan nanoparticles, by inhibiting NF- kB and consequent inhibition of pro-inflammatory cytokines and by playing a role on Bcl-2

downregulation (Abdel-Hakeem et al., 2021), and an upgrade compared to solely curcumin on characteristics like cellular uptake, cytotoxicity, pro-apoptotic activity (Arya et al., 2018).

There are also some studies where the potential for a synergistic effect, concerning both chitosan and curcumin inherent therapeutic effects previously mentioned, has been examined. The administration of curcumin-chitosan nanoparticles demonstrated a greater reduction in cadmium toxicity and associated oxidative stress on the kidneys and liver compared to individual administration (Ahmad et al., 2018). Furthermore, a synergistic effect against multidrug-resistant bacteria has been demonstrated (Etemadi et al., 2021) as well as against skeletal muscle fibrosis (Mahdy et al., 2022), a condition that shares certain pathological characteristics with HCC. In the latter article it was observed that the conjugation of both components led to a greater decrease in collagen deposition and inflammatory response compared to separate administration of the molecules, likely due to a combined inhibition of TGF-β1 signaling.

1.3.2 Functionalizing Chitosan Nanoparticles

The drug delivery systems have yet some obstacles to a more effective delivery of the drugs due to sometimes lacking specificity, which will culminate in low bioavailability in tissues and organs where it will be needed, and chitosan is no exception.

As previously mentioned, chitosan can be modified and functionalized primarily due to the presence of its amino and hydroxyl groups. (Jhaveri et al., 2021). More concisely, certain ligands, specific to a certain cell membrane receptor can be chemically linked on chitosan nanoparticles. This approach allows the delivery system to interact with the desired receptor and achieve a receptor-mediated endocytosis. There have been several studies regarding chitosan functionalization with different future prospects, ranging from the biomedical field to industrial and environmental applications (Pokhrel & Yadav, 2019).

In the particular case of HCC, there have been some recent studies that evaluate the potential enhancement of delivery of certain type of drugs, with functionalized chitosan nanoparticles. Two examples of the ligands are lactobionic acid and

glycyrrhetinic acid which have the ability to bind to surface receptors on hepatocytes and were used to deliver doxorubicin (Hefnawy et al., 2020). A similar approach was studied with hyaluronic acid modified chitosan to deliver paclitaxel (Puluhulawa et al., 2022). There is also an early study (W. J. Lin & Chen, 2007) that covers the attachment of galactose on chitosan nanoparticles, which successfully targeted ASGPR on hepatocytes, and another one (J. Wang et al., 2021) where the addition of galactose is mediated by the conjugation with lactobionic acid for the delivery of methotrexate to HepG2 cells' ASGPRs, which proved to have a higher cellular uptake than without the lactobionic acid (LA) modification, translating in a more effective antitumor activity.

Overall, this opens up a series of possibilities regarding active targeting of HCC using modified and functionalized chitosan nanoparticles.

1.4. Aim of the thesis

Nanotechnology has emerged as a promising approach in the pharmaceutical field, offering improved safety and efficacy of drug delivery systems. The objective of this thesis is to enhance the understanding of the impact of nanoparticles in drug delivery and immune response through the investigation of curcumin-encapsulated chitosan NPs. The study has four main goals:

- Preparation and characterization of curcumin encapsulated LA modified chitosan NPs.
- Investigation of the cytotoxicity of the NPs on both hepatocellular carcinoma cells and healthy immune cells.
- Assessment of the NP impact on oxidative stress in cancer cells to elucidate their antioxidant properties and potential therapeutic benefits.
- Evaluation of the immunomodulating capacity of the NPs to determine their ability to modulate immune responses and potentially enhance anti-tumor immunity.

Through these objectives, this study aims to contribute with valuable insights into the design and application of curcumin-encapsulated chitosan NPs for targeted therapy in hepatocellular carcinoma, paving the way for more effective and personalized cancer treatments.

Chapter 2 – Materials and Methods

2. Materials and Methods

2.1 Materials

Chitosan was obtained from Primex BioChemicals AS (Avaldsnes, Norway). Curcumin, lactobionic acid, MTT (3-(4,5-dimethylthiazol-2-yl)-2,5-diphenyltetrazolium bromide), TPP (tripolyphosphate), Dulbecco's modified Eagle medium (DMEM), Roswell Park Memorial Institute (RPMI) 1640, Fetal Bovine Serum (FBS), HEPES, Lipopolysaccharide (LPS), Concavalin A (ConA), were purchased from Sigma Aldrich Corp.

TNF-α and IL-6 ELISA kits were acquired from PeproTech (Rocky Hill, NJ, USA).

The human liver cancer cell line HepG2 was purchased from Sigma-Aldrich Corp. (St. Louis, MO, USA). The macrophages cell line Raw 264.7 was purchased from ECACC (Salisbury, UK).

Freshly drawn blood samples were kindly given by IPST IP (Coimbra, Portugal). The study was conducted in accordance with the Declaration of Helsinki, and the protocol was approved by the Ethics Committee of the Faculty of Medicine, University of Coimbra, Portugal (approval number: 063-CE-2019; date of approval: 24/06/2019).

All other chemicals used were from analytical grade.

2.2 Methods

2.2.1 Obtainment of LPS-free chitosan

The chitosan was subjected to a purification process described by Lebre et al., 2019 before being used in the production of nanoparticles and before being chemically modified with lactobionic acid. A mass of 1 g of medium molecular weight Chitosan (MW-CS) was dissolved in 10 mL of NaOH solution 1 M. The solution was agitated with a magnetic stirrer for 3 h at a temperature ranging between 40 ºC to 50 ºC. Next, the solution was filtered using a Buchner funnel and a paper filter. The chitosan was washed by adding 20 mL of Milli-Q water on top of the filter and then, dried. The chitosan was removed and dissolved in 200 mL of an acetic acid solution 1 % (w/v), using magnetic stirring for 1 h, at room temperature. The solution was again filtered by the same method, and the filtered solution was transferred to a

beaker. The pH was adjusted to around 8, with a solution of NaOH 1 M. It was then centrifuged for 30 min, at 4500 g. The supernatant was discarded, and the NPs were washed with Milli-Q water. Next it was vortexed and homogenized. The precipitated chitosan was centrifuged for 30 min at 4500 g, discarding again the supernatant and doing the same centrifugation conditions. The last supernatant was also discarded. The remaining pellet was frozen at -80 ºC for 24 h and it was then freeze-dried for 48 h. Afterwards, it was stored in the desiccator.

The method used to produce every type of nanoparticles on the present study was the inotropic gelation method. This method involves mixing the polymer solution (chitosan solution) with a cross-linking agent (tripolyphosphate) that forms a gel-like structure through ionic interactions.

2.2.2 Obtainment of LA-Chitosan

The production of the LA acid-chitosan polymer was done linking lactobionic acid to the amino group, as described by Bahadur K.C. et al., 2009. Briefly, the LPS-free Chitosan was mixed with Lactobionic acid (LA) in a ratio 10:10. The purified chitosan (93 % DD) was previously dissolved in acetic acid 1 % (V/V), stirring with a magnetic stirrer overnight. The pH was adjusted to around 4.7 using a 10 M NaOH solution. In order to activate the LA, 200 mg of it were dissolved, along with 128.5 mg of EDC (1-Ethyl-3-(3-dimethylaminopropyl)carbodiimide) and 77 mg of NHS (N-hydroxysuccinimide) in 20 mL of Milli-Q water for 1 h, under magnetic stirring. Then, 20 mL of LA solution were added dropwise to 10 mL of chitosan solution, under slow magnetic stirring and incubated for 24 h, at room temperature. A dialysis membrane was cut at 25 cm of length, and it hydrated for also 24 h, in 2 L of Milli-Q water under magnetic stirring. The resulting solution was dialyzed in 3 L of Milli-Q water, under magnetic stirring, for 72 h, with four replacements of the water (after 2.5 h, 18 h, 21 h and 26 h). The CS:LA solution was freeze-dried for 48 h twice, allowing the modified chitosan to thaw in between. The resulting LACS was stored in the desiccator.

2.2.3 Preparation of the nanoparticles

To produce the nanoparticles, two formulations were prepared: Chitosan Nanoparticles (CSNPs) and Lactobionic Acid-Modified Chitosan Nanoparticles

(LACSNPs). For both formulations, CS and LA-CS at 0.1% (w/v) were solubilized in an acetic acid 1% (w/v) solution overnight with a magnetic stirrer at 1000 rpm. The pH was adjusted by adding NaOH 10 M dropwise, until it reached values around 4.7. With the solution under an UltraTurrax rotation at a speed of 24000 rpm, the reagents were gradually added dropwise. First 200 µL of curcumin 0.25 % (w/v), followed by the addition of 1750 µL of TPP for CSNPs and 1000 µL for LACSNPs. The mixture was continuously rotated for 1 minute. Subsequently, magnetic stirring at 1000 rpm was employed for 30 minutes to facilitate the maturation of the nanoparticles. Afterwards, a centrifugation at 10000 x g for 20 min was done, with the supernatant being kept for encapsulation studies and the pellets resuspended in Milli-Q water. Next, a new centrifugation was performed, to clear the pellet of any undesirable substances, at 7000 x g for 15 min. The nanoparticles were stored in an Eppendorf tube at 4 ºC until used.

2.2.4 Characterization of nanoparticles' size and zeta potential

With a concentration of 10 mg/mL the NPs' suspensions were transferred to a cuvette where they were diluted following a ratio of 1:10 with Milli-Q water. The size was measured by dynamic light scattering (DLS) and the zeta potential was measured by electrophoretic light scattering (ELS) using a Zetasizer Nano ZS (Malvern Instruments, Ltd., Worcestershire, UK).

2.2.5 Evaluation of the degree of binding of lactobionic acid to the amine groups of the chitosan

The degree of binding of lactobionic acid to the amine groups of the chitosan was done by an indirect way, quantifying the free amine groups of chitosan before and after modification. The modification of chitosan with lactobionic acid occurs

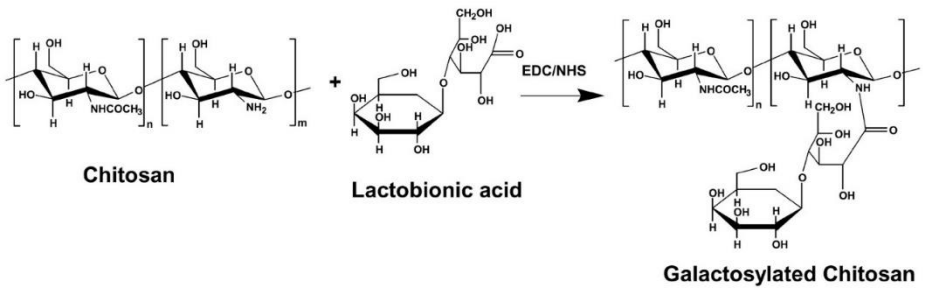

Figure 3. *The structural modification of Chitosan with Lactobionic Acid, through the addition of EDC and NHS.*

through a chemical reaction known as amidation, which involves the reaction between the primary amine groups (-NH2) of chitosan and the carboxylic groups (-COOH) of lactobionic acid (Figure 3).

The quantification of the amine groups was done performing the ninhydrin assay.

Ninhydrin reacts with the α-amino group of primary amino acids producing "Ruhemann's purple". The intensity of the color formed depends on the number and chemical nature of the amino groups being analyzed.

Both chitosan and lactobionic acid modified chitosan were dissolved in a 25 mM acetate buffer for 72 h at room temperature, under magnetic rotation and covered with parafilm. Next, 1 mL of the samples were added to 1 mL of 0.2 M acetate buffer and 1 mL of the ninhydrin solution on a 15 mL falcon, where they were mixed and incubated in a water-bath at 100 ºC for 20 min. Following this, the solutions were diluted with 6 mL of ethanol solution 60 %, from where 100 µL of each solution in triplicate was transferred to a non-sterile 96-well plate where the absorbance was read at 570 nm.

Free amino group concentrations could be interpolated from a standard curve prepared with glycine standards. However, assessing the evaluation of free amino groups in the chitosan polymer using this methodology is difficult because some amino groups may not be accessible for reaction and measurement. Due to this limitation, it was decided to present the results as a ratio (Equation 1) between the optical density (OD) of the LA modified chitosan and the OD of the original chitosan after the reaction with the Ninhydrin reagent.

$$Free\ Amine\ Groups\ (\%) = \frac{\text{OD A}_{570}(LA\ modified\ Chitosan) \times 100}{\text{OD A}_{570}(Chitosan)}$$

(Equation 1)

2.2.6 Quantification of Curcumin

To calculate the efficiency of curcumin encapsulation into chitosan NPs, the quantification of non-encapsulated curcumin present in the supernatant of each suspension of the nanoparticles was done. The suspension was centrifuged at 7000

x g and the supernatant was separated from the pellet. The supernatant was subjected to a new centrifugation at a higher speed (21000 x g) for another 10 min.

Due to its intrinsic yellow color, the measurement of curcumin was simply performed using an UV-Vis spectrometer. The optical density (OD) of this second supernatant was immediately measured at 426 nm wavelength, after its separation.

Curcumin concentrations were obtained by the interpolation from a calibration curve prepared with the curcumin standards with concentrations ranging from 0 µg/mL to 4.18 µg/mL.

2.2.7 Stability of Nanoparticles

All the different nanoparticles were stored, in triplicate, at three different temperatures: 4 ºC, 20 ºC and 37ºC. During a month, their size, PDI and ZP were measured using the Zetasizer Nano ZS (Malvern Instruments, Ltd., Worcestershire, UK). From the same initial nanoparticle suspension, they were divided onto 3 Eppendorf stored at the temperatures mentioned. Measurements were performed at days 0, 1, 3, 10, 15 and 30.

2.2.8 Effect of nanoparticles on cytotoxicity and ROS production of HepG2 Cell line

HepG2 cells were cultured with DMEM (Dulbecco's Modified Eagle Medium) supplemented with 10 % FBS (fetal bovine serum), 1 % PenStrep, 10 mM HEPES, 12 mM sodium bicarbonate in a humidified atmosphere, with 5 % CO_2, at 37 ºC.

To evaluate the cytotoxicity of all nanoparticles on HepG2 cells, a protocol was followed as described in the literature. Briefly, 100 µL of HepG2 cells were plated in a 96-well plate at a density of 6 x 10^5 cells/mL and incubated overnight at 37 ºC with 5 % CO_2. The cell culture medium was removed, and 150 µL of DMEM and 50 µL of our nanoparticles' formulation (table 1) were added to each well, accounting for a negative control. The plate was then incubated for 24 h at 37 ºC with 5 % CO_2. Afterwards, the cell culture was removed and 200 µL of a resazurin solution with serum-free DMEM (10 µL to 15 mL) was added to each well and incubated at 37 ºC for 2 h. The plate was read at 570 nm and 620 nm. The relative cell viability (%) was

calculated in relation to the control (cells in culture medium), as described on the following equation (Equation 2).

$$Cell\ Viability\ (\%\ of\ control) = \frac{OD\ sample\ (540\ nm) - OD\ (630\ nm)}{OD\ control\ (540\ nm) - OD\ (630\ nm)} \times 100$$

(Equation 2)

While performing the cell viability assay, it was also possible to measure ROS production. After the incubation with the nanoparticles and removal of the medium, 200 µL of a solution of dichlorofluorescein diacetate (DCFH-DA) in serum-free DMEM (20 µL to 20 mL) would be added to each well, except for the negative control without probe, which still received 200 µL of only serum-free DMEM. The plate was then incubated for an additional 1 h at 37 ºC and 5 % CO_2, in the absence of light. Finally, the resulting fluorescence was read at 485/20 nm (excitation wavelength) and 528/20 nm (emission wavelength). The calculations followed Equation 3, which aimed to determine Fluorescence Increase Fold.

$$Fluorescence\ Increase\ Fold = \frac{F\ sample - F\ Control\ without\ probe}{F\ Control\ with\ probe - F\ Control\ without\ probe}$$

(Equation 3)

Table 1. *Concentrations of NPs and curcumin tested on HepG2 cells to determine cell toxicity.*

[Chitosan] (µg/mL)				**[Curcumin] (µM)**	
CSNP	**CSCNP**	**CSLANP**	**CSCLANP**	**CSCNP**	**CSCLANP**
187.5	187.5	187.5	187.5	0.184	0.184
375	375	375	375	0.368	0.368
750	750	750	750	0.736	0.736
1500	1500	1500	1500	1.47	1.47

CS: Empty Chitosan Nanoparticles; CSC: Curcumin-Encapsulated Chitosan Nanoparticles; CSLA: Empty Lactobionic Acid-modified Chitosan Nanoparticles; CSCLA: Curcumin-Encapsulated Lactobionic Acid-modified Chitosan Nanoparticles

2.2.9 Effect of nanoparticles on cytotoxicity and ROS production of Raw 264.7 Cells

Raw 264.7 cells were cultured with DMEM (Dulbecco's Modified Eagle Medium) supplemented with 10 % FBS (fetal bovine serum), 1 % PenStrep, 10 mM HEPES, 12

mM sodium bicarbonate and 11 mg/mL sodium pyruvate in a humidified atmosphere, with 5 % CO_2, at 37 ºC.

To evaluate the cytotoxic effects of CSNPs, RAW 264.7 cells were seeded at a density of 2 x 10^5 cells/mL in a 96-well plate and incubated for 24 h. The culture medium was then removed, and 150 µL DMEM was added to the cells which were treated with the addition of 50 µL of our nanoparticles diluted in water, following concentrations displayed on table 1, for a set time period.

Some controls were included to account for any effects of the solvent or vehicle used. After treatment, the medium was removed, and 200 µL of serum-free DMEM was added to the cells, which were incubated with 20 µL more of an MTT solution for 1 h and 30 min. The resulting formazan crystals were dissolved in 200 µL DMSO and 25 µL of glycine buffer, and the absorbance was measured at 540 nm and 630 nm. The relative cell viability was calculated as a percentage of the control cells incubated in medium only, as described on Equation 2.

As to assess ROS production, the same conditions were followed, but after the incubation with the nanoparticles and removal of the medium, 200 µL of 50 µM dichlorofluorescein diacetate (DCFH-DA) probe in serum-free DMEM was added to each well (except for the negative control without probe, which received 200 µL of serum-free DMEM). The plate was then incubated for 2 h at 37 ºC and 5 % CO_2. The resulting fluorescence was read at 485/20 nm (excitation wavelength) and 528/20 nm (emission wavelength) using a microplate reader. The calculations followed Equation 3.

2.2.10 Effect of nanoparticles on splenocytes' cytotoxicity

Splenocytes were isolated from spleens that were removed from CD1 mice. The splenocytes were cultured with RPMI 1640 (Roswell Park Memorial Institute) cell culture medium supplemented with 10 % (v/v) FBS, 2 mM glutamine, 1 % (v/v) PenStrep and 20 mM HEPES buffer.

Mice were sacrificed by cervical dislocation 2and their spleens were aseptically removed. Next, they were transferred to 15 mL centrifuge tubes with 5 mL of T cell media (RPMI 1640 R6504). The spleens were dissociated with cell strainers (70 µm) into a 50 mL tube followed by the addition of 3 mL of T cell media to wash the cell

strained. Spleen cells were spun at 220 x g for 10 min in at 4 ºC and their supernatant was removed. The pellet was then resuspended, and 0,5 mL of ACK lysing buffer were added. For 2 min the tube was placed on ice. Then, it was filled with 10 mL of T cell media and the cells were mixed. A centrifugation at 220 x g for 10 min at 4 ºC was followed, where the supernatant was discarded, and the pellet resuspended in 10 mL of T cell media with serum (10 % FBS). The cells were once again centrifuged at the previous conditions and resuspended in 4 mL of T cell media with serum and cell count was followed.

A volume of 50 µL of spleen cells were plated at a concentration of $1x10^7$ cells/mL. Next, 125 µL of media were added as well as 25 µL of our NPs, following concentrations displayed at table 2. Following 96 h of incubation the supernatants were removed and 200 µL of resazurin in media (15 µL to 20 mL) were added for an overnight incubation at 37 ºC. The plate was then read at 570 nm and 620 nm. The relative cell viability was calculated as a percentage of the control cells incubated in medium only, as described on Equation 4.

Table 2. *Concentrations of NPs and curcumin tested on splenocytes to determine cell toxicity.*

[Chitosan] (µg/mL)				**[Curcumin] (µM)**	
CS	**CSC**	**CSLA**	**CSCLA**	**CSC**	**CSCLA**
5	5	5	5	0.0049	0.0049
40	40	40	40	0.0392	0.0392

CS: Empty Chitosan Nanoparticles; CSC: Curcumin-Encapsulated Chitosan Nanoparticles; CSLA: Empty Lactobionic Acid-modified Chitosan Nanoparticles; CSCLA: Curcumin-Encapsulated Lactobionic Acid-modified Chitosan Nanoparticles

$$Cell\ Viability\ (\%\ of\ control) = \frac{OD\ sample\ (570\ nm) - OD\ (620\ nm)}{OD\ control\ (570\ nm) - OD\ (620\ nm)} \times 100$$

(Equation 4)

2.2.11 Effect of nanoparticles on cytotoxicity on PBMCs

PBMCs were isolated from freshly drawn blood, which was kindly given by IPST IP (Coimbra, Portugal) and isolated on a density gradient with Lymphoprep™ (Axis-Shield, Dundee, Scotland).

Starting from the PBMCs tube that were extracted from the neutrophil isolation, the cells were washed by adding an excess of HBSS and centrifuging for 10 min at 400 x

g, at 20 ºC. The volume of HBSS used was approximately three times the volume of the mononuclear layer. The supernatant was discarded, and the wash step was repeated once more. Finally, the cells were resuspended in complete RPMI-1640 medium.

First, the cell concentration was adjusted to 1 x 10^6 cells/mL using complete RPMI medium. Then, a volume of 100 µL of both the control samples and the nanoparticle samples were dispensed into each well of a 96-well plate, following NPs' concentrations displayed at table 2. To ensure proper mixing, 100 µL of the cell suspension or cell culture medium (for cell-free controls) was added to each well, followed by gentle shaking of the plate. The plate was then incubated in a humidified 37 ºC, 5 % CO_2 incubator for 24 ± 2 h.

After incubation, the plate was centrifuged at 700 x g for 5 min, and the medium was carefully aspirated, leaving the cells behind. 100 µL of fresh medium was added to each well, and the plate was gently tapped to mix the components. Subsequently, 100 µL of PHA-M working solution was added to the original plate containing 100 µL of cell suspension, except for the wells with untreated cells. The plate was covered and incubated for 72 h ± 2 h in a humidified 37 ºC, 5 % CO_2 incubator. After the incubation period, the plate was centrifuged again at 800 x g for 20 min, and the medium was aspirated. Fresh medium (150 µL) was added to each well, and the plate was gently tapped to mix the components. To assess cell viability further, 50 µL of MTT solution was added to all wells. The plate was covered with aluminum foil and incubated in a humidified 37 ºC, 5 % CO_2 incubator for 4 h. Following incubation, the plate was removed from the incubator and spun at 800 x g for 20 min. The media and MTT solution were aspirated, and 200 µL of DMSO was added to all wells. Additionally, 25 µL of glycine buffer was added to each well to ensure solubilization of formazan crystals. For measurement purposes, 200 µL of the plate contents were transferred to a 96-well flat bottom plate. If the plate reader allowed for round bottom plates, this transfer step could be skipped. Finally, the plate was read at 570 nm and 620 nm on a plate reader to evaluate cell viability, which was calculated following Equation 4.

2.2.12 Effect of nanoparticles on neutrophils' cytotoxicity and ROS production

Neutrophils were isolated from freshly drawn blood, which was kindly given by IPST IP (Coimbra, Portugal) and isolated on a density gradient with Lymphoprep™ (Axis-Shield, Dundee, Scotland).

With the buffy coat sterilized, the blood was divided into 50 mL tubes, with 30-35 mL of blood in each tube. An initial centrifugation at 1100 x g for 10 min was done, with no break, from where the upper layer was discarded. Next, PBS 1x was added until a final volume of 50 mL, and the mixture was homogenized by inversion. Next, 10 mL of Lymphoprep™ were added, dropwise, beneath the blood layer, keeping the density gradient medium and remaining buffy coat separate. The tubes were centrifuged at 1100 x g for 20 min without brake, allowing the formation of distinct layers: a top layer of serum/plasma, a middle white ring of Peripheral Blood Mononuclear Cells (PBMCs), a cloudy density gradient medium layer, and a bottom pellet consisting of a white, thin band of neutrophils on top of the Red Blood Cells (RBCs). The top layer was discarded, and the PBMCs were transferred to a new tube, while the neutrophil/RBC layer was transferred to another clean tube.

The erythrocyte sedimentation process involved transferring the neutrophil/ RBC pellet into a clean tube. To this, 5 % FBS/HBSS solution was added to achieve a final volume of 25 mL. Another 25 mL of a prewarmed (37 ºC) solution containing 3 % dextran/0.9 % NaCl in water was directly added to the tube and gently mixed by inversion. The tube was then placed on a leveled and non-vibrating surface for 15 min. After returning the tube to the hood, approximately 30 mL of the top layer was collected by slightly immersing the pipette in the liquid and following the liquid surface downwards. Afterwards, it was spun in order to obtain a red pellet without floating particles in the media.

To lyse residual RBCs, the supernatant was gently aspirated without disturbing the pellet, and 25 mL of sterile ultrapure water were added to the tube, followed by gentle mixing for 28 seconds. Immediately after, 25 mL of sterile 1.8 % NaCl solution prepared in water were added to restore isotonic conditions through gentle mixing. The tube was spun at 200 x g for 3 to 5 min with a low brake to minimize the sedimentation of RBCs and platelets with neutrophils. To resuspend the white

neutrophil pellet, culture medium was directly added without pipetting up and down, and the tube was gently rocked horizontally to minimize cell activation.

In case of observed cell aggregation or clumping, the cell suspension was filtered through a 70 μm mesh to remove clumped neutrophils.

A volume of 100 μL of neutrophils at a concentration of 2x10^6 cells/mL were plated in 96 well plates and incubated for 2 h. Following this, 50 μL of RPMI medium and 50 μL of nanoparticle solutions were added, following concentrations displayed at table 2, including both positive and negative controls. The cells were then incubated for an additional 2 h and the supernatant were discarded. To assess cell viability, 200 μL of resazurin in media (prepared by adding 15 μL of resazurin to 20 mL of media) were added, and the plate was incubated overnight at 37 ºC. Finally, the plate was read at 570 nm and 620 nm, and the relative cell viability (%) was calculated by comparing the results to the control group of cells cultured in the medium alone, as described on Equation 4.

To evaluate ROS production, 20 μL of ROS probe in medium were previously added to the cells, resulting in a final concentration of 30 μg/mL, and they were incubated for another 1 h. Following this, 50 μL of medium and 50 μL of nanoparticle solutions were added. A positive control was included using LPS at a concentration of 2 μg/mL, and a negative one with and without the probe. The cells were then incubated for an additional 2 h. Subsequently, the cells were centrifuged at 200 x g for 10 min, and the supernatant was transferred to a black plate to measure ROS production, following the same measurements as for HepG2 and Raw264.7, and using Equation 3.

2.2.13 Effect of the formulations on the production of TNF-α and IL-6 by splenocytes

The samples used to perform this experiment were the supernatants previously separated from spleen cells, during viability assay, and kept at -80 ºC.

A volume of 50 μL of spleen cells had been incubated with 40 μg/mL and 5 μg/mL of chitosan, corresponding to 0.049 and 0.0049 μM of curcumin respectively, at a concentration of $1x10^7$ cells/mL, with 125 μL of media and 25 μL of the NPs. Following 96 h of incubation the supernatants were extracted and freeze at -80 ºC.

For the cytokine quantification, sandwich ELISAs were performed according to the kits' vendor's protocols (PeproTech®).

2.8 Statistical Analysis

The data were analyzed using GraphPad Prism 8 software (GraphPad Software, Inc., La Jolla, CA, USA). To determine significant differences between the samples, Student's t-tests were performed. This allows for comparison between the means of two groups to identify any statistically significant differences between them.

Chapter 3 – Results and Discussion

3. Results and Discussion

3.1 Production and Characterization of Nanoparticles

The first goal of this thesis work was to produce different types of curcumin-loaded nanoparticles, to use in various cellular assays. These nanoparticles were divided into four types:

- Chitosan Nanoparticles (CSNPs).
- Chitosan Nanoparticles encapsulated with Curcumin (CSCNPs).
- Lactobionic Acid-Modified Chitosan Nanoparticles (LACSNPs).
- Lactobionic Acid-Modified Chitosan Nanoparticles encapsulated with Curcumin (LACSCNPs).

Biological studies using these different formulations allowed us to determine whether the observed effects were due to the encapsulation of curcumin. The use of empty nanoparticles enabled a comparison of the effects of chitosan nanoparticles alone with those resulting from the combination of both compounds. The same logical approach was applied to the modified chitosan, as it was important to assess any possible variations that could arise from the association of lactobionic acid to chitosan to obtain a chitosan derivative.

The preparation method underwent several adjustments to ensure reproducibility between batches and to obtain particles with a small size and low polydispersity index (PDI). The characteristics of the final nanoparticle formulation, such as size, polydispersity index (PDI), and zeta potential (ZP), were measured and discussed.

The effective modification of the chitosan, as well as the proper encapsulation of curcumin were also evaluated.

3.1.1 Chitosan and LA-modified chitosan nanoparticles were successfully produced and characterized

The chemical modification of chitosan involved the introduction of lactobionic acid (LA) into the polymer. This modification was achieved by the reaction between the carboxyl group of LA and the free amine groups of chitosan, resulting in the formation of an amide bond and reducing the availability of free amine groups (Bahadur K.C. et al., 2009). The degree of deacetylation of chitosan is an important

parameter, as it influences the physical, chemical, and biological properties of the polymer. Additionally, this modification through lactobionic acid conjugation leads to a decrease in the percentage of free amine groups. To assess the success of this chemical modification, the ninhydrin assay was employed to quantify the remaining free amine groups in chitosan after the linkage with lactobionic acid.

Considering the original polymer as having 100 % of predicted amine groups and making a comparison with the modified chitosan, it is observed that there was a decrease in free amine groups and the value found was 63.72 % ± 1.71 % (± SEM) (Figure 4A). This value demonstrates that some amine groups were used to link to LA and proves by an indirect way that the chitosan was modified. The values recorded are similar to the ones documented by Wei et al., 2017, where it was observed a decrease of 40.1 % of free amine groups.

The results of curcumin encapsulation efficiency (EE), in both types of chitosan nanoparticles were depicted in figure 4B: chitosan NPs registered a mean curcumin encapsulation efficiency of 86.98 % ± 1.9 % (± SEM) and the lactobionic acid-modified chitosan NPs had EE of 86.67 % ± 3.0 % (± SEM).

Physicochemical properties of nanoparticles have direct influence on the desired biological effects. The mean diameter of the different types of particles were resumed in figure 4C. The CSNP registered a size of 368.92 ± 39.24 nm, CSCNP with 400.88 ± 46.09 nm, LACSNP had 399.95 ± 11.64 nm and for LACSCNP the size was 408.8 ± 27.69 nm. The increase in size when comparing curcumin-loaded with empty CS and LACS nanoparticles was expected due to the introduction of curcumin in the production of NPs.

The polydispersity index (PDI), a representation of the distribution of size populations within a given sample was described in figure 4C. The values were considerably high. Although there weren't significant differences between three of the four nanoparticles (CSNP registered a PDI of 0.436 ± 0.042, CSCNP of 0.429 ± 0,033, and LACSCNP of 0.421 ± 0.04). Nevertheless, the PDI value used as a guideline is below 0.07 (International Organization for Standardization [ISO], 2017, 22412:2017), indicating a monodisperse sample with a narrow size distribution. These high values of PDI might have coursed due to particle aggregation. To try to

avoid this, the NPs suspensions underwent ultrasound bath treatment, for different time periods (3, 5 and 12 min) before measuring the size during tryouts for optimization, but the results produced with sonication didn't show any improvement.

The Zeta Potential (ZP) of the different nanoparticles were similar: CSNP with +43.06 ± 0.64 mV, CSCNP had +42.03 ± 0.62 mV, LACSNP had +43.81 ± 1.06 mV and LACSCNPs +43.5 ± 1.78 mV. All these values indicate a relatively high positive surface charge. Although having very small differences, the small increase in voltage, comparing CS and LACS nanoparticles was not expected. Lactobionic acid binds to free amine groups which are positively charged, through amide bonds, which should decrease the overall ZP (J. Wang et al., 2021). There is also a pattern regarding the addition of curcumin, that shows a small decrease in ZP value of nanoparticles containing it, when comparing that measurement with the empty ones.

Considering the best possible outcome of this work, which is the use of these nanoparticles in future *in vivo* experiments, it becomes crucial to explore their storage options. Long-term storage may be necessary to avoid frequent production, and in an optimistic scenario, transportation and extended storage periods might be involved. Therefore, understanding the optimal conditions for achieving the best shelf-life is essential. To assess the stability of the formulations, a 30-day stability test was conducted, subjecting the nanoparticles to different temperatures. Throughout this test, measurements of nanoparticle size, Polydispersity Index (PDI), and Zeta Potential (ZP) were taken over time. The goal was to determine the most suitable temperature for storing the nanoparticle suspensions until they are used in subsequent biological studies. The results obtained can be observed in figure 4D, regarding the particles' diameter, figure 4E, for the final PDI and figure 4F for the final ZP. Within a month, we can see that, overall, nanoparticles that were stored at 4ºC didn't have any significant variations to its size. Meanwhile, those that had been stored either at room temperature (20 ºC) or at 37 ºC had significant changes in their diameter. This goes along to what was expected, according to literature (Morris et al., 2011) about hollow chitosan nanoparticles. Also, there didn't seem to be an accentuated difference on size, when comparing simple chitosan NPs or lactobionic acid-modified chitosan NPs with the curcumin loaded chitosan NPs with

LA associated or not to the particles. However, particles with LA showed a tendency to possibly aggregate more at 20 ºC and 37 ºC temperatures, having a higher final PDI value.

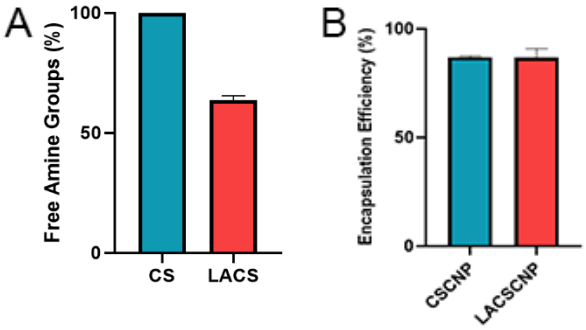

C

Nanoparticle	Diameter (nm) ± SD	PDI ± SD	ZP (mV) ± SD
CSNP	368.92 ± 39.24	0.436 ± 0.042	43.06 ± 0.64
CSCNP	400.88 ± 46.09	0.429 ± 0.033	42.03 ± 0.62
LACSNP	399.95 ± 11.64	0.380 ± 0.089	43.81 ± 1.06
LACSCNP	408.8 ± 27.69	0.421 ± 0.04	43.5 ± 1.78

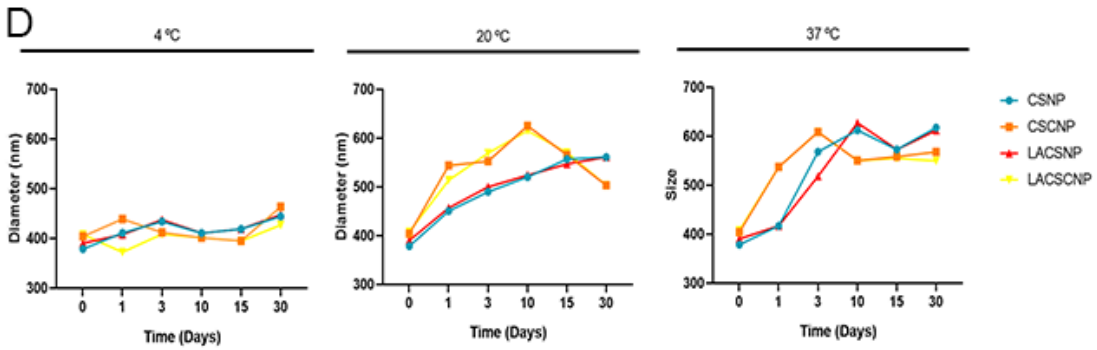

E

	PDI ± SEM		
	4 ºC	20 ºC	37 ºC
CSNP	0.36 ± 0.054	0.36 ± 0.006	0.38 ± 0.013
CSCNP	0.35 ± 0.046	0.38 ± 0.018	0.40 ± 0.004
LACSNP	0.31 ± 0.039	0.32 ± 0.016	0.34 ± 0.012
LACSCNP	0.34 ± 0.029	0.36 ± 0.023	0.37 ± 0.006

F

	Zeta Potential ± SEM		
	4 ºC	20 ºC	37 ºC
CSNP	40.01 ± 0.22	37.91 ± 0.3	37.12 ± 1.41
CSCNP	40.53 ± 0.18	37.87 ± 0.21	36.3 ± 0.95
LACSNP	41.79 ± 0.15	39.43 ± 0.33	36.68 ± 1.12
LACSCNP	41.11 ± 0.07	39.66 ± 0.29	36.09 ± 1.34

Figure 4. *Physicochemical description of hollow and curcumin containing nanoparticles.* ***(A)*** *Estimated percentage of free amine groups, calculated using Equation 1, in a chitosan solution (CS) and lactobionic acid modified chitosan solution (LACS). The data were presented as the mean ± SEM, n = 3 (three independent experiments, each in triplicate).* ***(B)*** *Percentage of curcumin encapsulated into chitosan and LA-chitosan nanoparticles (CSCNP and LACSCNP, respectively). The data were presented as the mean ± SEM, n = 3 (three independent experiments, each in triplicate).* ***(C)*** *Values of the mean ± SD regarding size distribution, polydispersity index (PDI), and zeta potential (ZP), n = 5 (five independent experiments, each in triplicate).* ***(D)*** *Influence of different temperatures during storage on NPs' size stability for 30 days – 4 ºC (left), 20 ºC (middle) and 37 ºC (right). Data were presented as the mean, n = 3 (three independent experiments, each in triplicate).* ***(E)*** *NPs' PDI values after 30 days of conservation at 4 ºC, 20 ºC and 37 ºC. The data were presented as the mean ± SEM, n = 3 (three independent experiments, each in triplicate).* ***(F)*** *NPs' ZP values after 30 days of conservation at 4 ºC, 20 ºC and 37 ºC. The data were presented as the mean ± SEM, n = 3 (three independent experiments, each in triplicate).*

3.2 Biological assays

The scientific community tends to believe that curcumin has a high therapeutic potential. However, its low solubility and consequent bioavailability have prevented this naturally occurring molecule from being more widely used. A strategy to increase its bioavailability is its encapsulation in nanoparticles.

The thesis aimed to investigate the effect of the encapsulation of the curcumin into LA modified chitosan NPs and chitosan NPs on cells. To this purpose the cell viability was studied with two cell lines, HepG2 cells, which is an epithelial hepatocellular carcinoma human cells, and RAW 264.7 which is a macrophage cell line extracted from a tumor in a male mouse. Apart from these two cell lines, three other primary cells were used: spleen cells from mice, human PBMCs (Peripheral Blood Mononuclear Cells) and human neutrophils, that were extracted from blood of a human donor (buffy coat).

The choice of HepG2 cells is essential since the study focuses on determining the effect of NPs on hepatocellular carcinoma cells. Substituting Kupffer cells, which form a dense population of macrophages in the liver and play a vital role in maintaining liver functions (Nguyen-Lefebvre & Horuzsko, 2015), with RAW 264.7 cells was crucial for this study's experimental design. Although the use of Kupffer cells in this research was not feasible, RAW 264.7 cells served as a suitable substitute for investigating macrophage-related processes. The splenocytes were chosen because the spleen is an organ of the immune system and constitutes a good representative of the cells of the immune system, easy, simple, and cost-effective to obtain. Finally, human cells were used too, in order to be able to have data closer to what could happen in terms of safety in clinical trials.

In this regard was used the Peripheral Blood Mononuclear Cells (PBMCs), a key component of the immune system, that includes various types of immune cells such as lymphocytes (70 % - 90 %), monocytes (10 % - 20 %) or dendritic cells (1 % - 2 %) (Kleiveland, 2015), responsible for recognizing and eliminating cancer cells. Finally, the neutrophils were used too to test formulations since they are a type of white blood cells that play a critical role in the body's immune response to infection and inflammation (S. L. Zhou et al., 2016).

Firstly, cell viability tests were carried out with each of the cell lines to ensure that a concentration of nanoparticles considered cytotoxic would not be used in the following tests. After evaluating the cell viability, the investigation shifted towards examining the impact of the curcumin encapsulated into NPs on oxidative stress of HepG2, RAW 264.7 cells and neutrophils. In this respect, it is also important to mention that studies exploring the inhibitory capacities of the NPs were not performed, as it would imply a combined LPS and NPs incubation. LPS would stimulate ROS production and NPs could show the ability to counterbalance this effect. However, the results coming from this hypothesis wouldn't be truthful as chitosan binds LPS through electrostatic interactions (Yang et al., 2021), which wouldn't allow for LPS to proper stimulate the cells.

3.2.1 The encapsulation of the curcumin maintains the high cellular viability in HepG2 cells and decreases ROS production

HepG2 cells were incubated for 24 h in 96 well microplates with the four types of nanoparticles, as well as free curcumin and a negative control, in order to have their cell viability measured through the resazurin assay. The results were depicted in figure 5A. None of the tested nanoformulations showed a decrease of cell viability using HepG2 cells, independently of the range of concentrations of both curcumin and chitosan that were used.

There wasn´t any significant difference. With this result, the assay to verify ROS stimulation by cells could be tested with any of the previously tested concentrations.

The evaluation of ROS production by cells, in this case HepG2 cells, is important due to its direct correlation with oxidative stress.

The ROS evaluation assays were conducted using the same formulation concentrations and incubation period of 24 h as previous observed with cell viability. By performing the ROS measurements after assessing cell viability, it allows for a sequential evaluation of cellular responses and provides insights into the potential role of oxidative stress in the observed effects of NPs on HepG2 cells. So, cells were incubated with a DCFH-DA probe for 1 h, after previously being incubated for 24 h with the formulations.

The results illustrated in figure 5, showed differences between particles loaded with curcumin and without curcumin.

When looking at the non-encapsulated curcumin results, we see that the four tested concentrations make up the four groups with the highest decrease in ROS production, with this decrease being clearly concentration-dependent, with the highest recorded value of decrease being the non-encapsulated curcumin at 1.47 µM. This information confirms that curcumin is indeed able to decrease ROS production, conforming its antioxidant role, as suggested by literature (Chen et al., 2020).

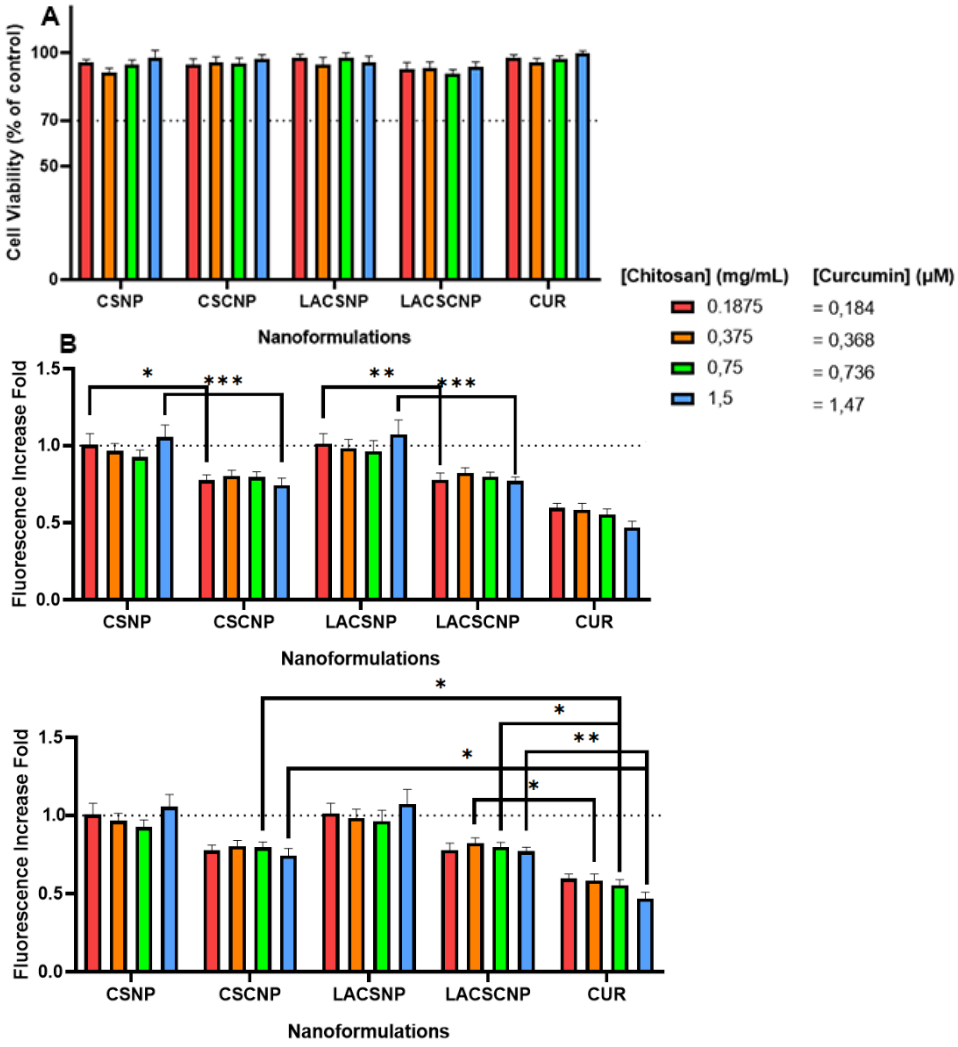

Figure 5. *Results regarding the effect of the nanoformulations on HepG2 cell viability and ROS production. CSNP: Empty Chitosan Nanoparticles; CSCNP: Curcumin-Encapsulated Chitosan Nanoparticles; LACSNP: Empty Lactobionic Acid-modified Chitosan Nanoparticles; LACSCNP: Curcumin-Encapsulated Lactobionic Acid-modified Chitosan Nanoparticles; CUR: Free, non-encapsulated curcumin* ***(A)*** *Evaluation of cell viability displayed by the HepG2 cell line, after a 24 h incubation with all nanoparticles and free curcumin.* ***(B)*** *Induction of ROS production by HepG2 cells after 24 h of incubation with all nanoparticles and free curcumin. Error bars represent SEM. (N=6; six independent assays, each in triplicate). (* = $p < 0.05$).*

By comparing both figure 5A and figure 5B, there seems to be no relation between ROS inhibition or production and the viability observed on the HepG2 cell culture, meaning that the encapsulation of curcumin did not affect cell viability.

Both types of nanoparticles containing curcumin (CSCNP and LACSCNP), have a downgrade regarding ROS production. This indicates that curcumin didn't lose its antioxidant effect, even though being constricted within chitosan. When encapsulated, the values of ROS production don't directly look like being concentration dependent. There is a clear difference on ROS production when comparing free, non-encapsulated curcumin, and NPs containing it. The latter do not provoke such strong decrease on ROS production, despite the concentration of curcumin being the same. Hollow chitosan nanoparticles (CSNP and LACSNP) don't seem to induce nor reduce ROS production, as the values of fluorescence are similar to the untreated control, despite having some spikes above 1.0 threshold. With this being said, the differences observed between ROS production of free curcumin and encapsulated-curcumin nanoparticles may be due to different factors, like a slow release of curcumin or even a small incapacity of fully delivering the compound.

It is also visible that expressing lactobionic acid on chitosan's surface, didn't directly translate to a more significant or noticeable effect in any of the assays. CSNPs and CSCNPs have very close results to LACSNPs and LACSCNPs on cell viability, respectively, which could have not been the case.

3.2.2 Nanoparticles achieved good values of viability in Raw 264.7 cells and a disparity on its effects regarding ROS production

Raw 264.7 cells were incubated for 24 h in 96 well microplates with the four types of nanoparticles, as well as free curcumin and a negative control, in order to have their cell viability measured through the MTT assay. The results are displayed in figure 6A.

When comparing the results observed in figure 5A to the ones displayed on figure 6A, there are some aspects that allow for a more effective characterization of the graphs.

There is a small decrease in cell viability, despite not going under 70 % in any of the cases. Although not having statistically significant differences, LACSNPs achieved

the lowest values of viability and there also seems to exist some influence of curcumin on cell viability, as both types of NPs containing curcumin have higher viability than their hollow counterparts.

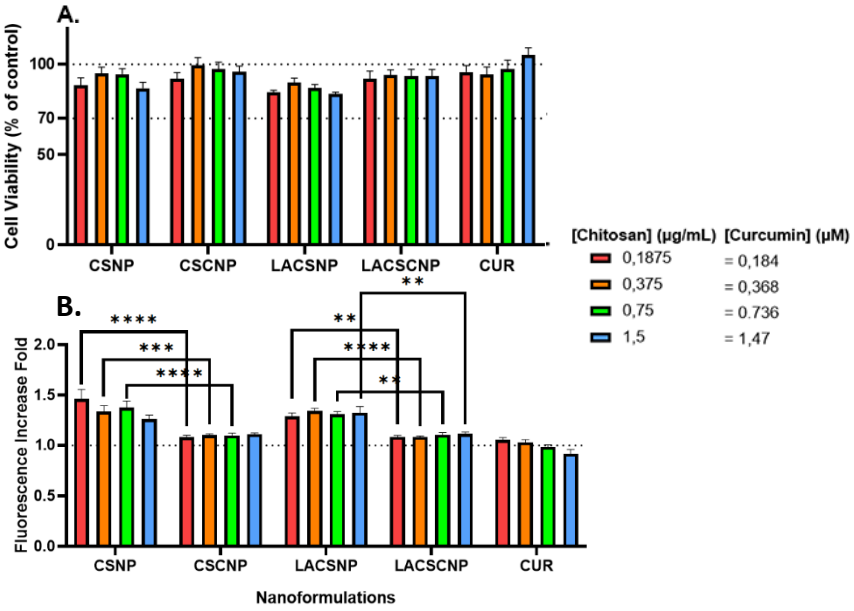

Figure 6. *Results regarding the effect of the nanoformulations on Raw 264.7 cell viability and ROS production. CSNP: Empty Chitosan Nanoparticles; CSCNP: Curcumin-Encapsulated Chitosan Nanoparticles; LACSNP: Empty Lactobionic Acid-modified Chitosan Nanoparticles; LACSCNP: Curcumin-Encapsulated Lactobionic Acid-modified Chitosan Nanoparticles; CUR: Free, non-encapsulated curcumin.* ***(A)*** *Evaluation of cell viability displayed by the Raw 264.7 cell line, after incubation with all nanoparticles and free curcumin.* ***(B)*** *Induction of ROS production by Raw 264.7 cells after 24 h of incubation with all nanoparticles and free curcumin. (N=4; four independent assays, each in triplicate). Error bars represent SEM. (* = $p < 0.05$)*

Even though the highest concentration of free curcumin shows the highest values of cell viability, the same doesn't apply to the encapsulated curcumin, independently of the type of nanoparticle used. This can be due to the fact that, in order to administrate the same amount of encapsulated curcumin as free curcumin to Raw 264.7 cell line, we need to increase the amount of chitosan – 1.5 mg/mL despite not having any natural toxic effects, chitosan can still be an obstacle to cell viability on the conditions described, as at higher concentrations it may induce some cytotoxic effects on RAW 264.7 cells, due to possible sedimentation on the medium, not allowing for cell proliferation.

Oxidative stress in macrophages plays a dual role in cancer, especially in the tumor microenvironment: if we can have controlled values of ROS it is possible to inhibit tumor growth, while excessive ROS production can promote tumor progression, so

its highly important to control this balance in macrophages for effective cancer therapy.

With this in mind, the following step was to assess ROS production in Raw 264.7 cells, as it has a direct connection to oxidative stress. Cells were incubated with a DCFH-DA probe for 2 h, after previously being incubated for 24 h with the formulations.

The results on figure 6B have some coincidences with the ones registered for HepG2 cells on figure 5B, regarding the roles of chitosan and curcumin. Free curcumin, which previously had a significant impact on the decrease of ROS production, here doesn't seem to be as effective, although it still shows a decrease to some extent at its highest concentration. With this being said, at the tested concentrations, curcumin is not closely as effective in this regard as it was for HepG2 cells.

When curcumin is encapsulated, it achieves very close values to the ones registered for the free curcumin. Despite not being able to decrease ROS production, it can influence it and bring it down to around control-levels. All four curcumin concentrations produce closely the same effect on ROS production, whether its encapsulated on chitosan or in modified chitosan nanoparticles, with no significant differences observed. The empty chitosan nanoparticles (CSNP) also have the highest production of ROS, being followed by LACSNP, which is not as high. This might indicate a stimuli of ROS production, induced by chitosan. This same effect is not observed on the curcumin-containing NPs, meaning that curcumin can counterbalance the effect of chitosan. On Raw 264.7 cells, these hollow nanoparticles proved to have a more impacting effect, with its increase in ROS production being more significant than the small peaks observed on HepG2.

By comparing both figure 6A and figure 6B, we can see a tendency. CSNP and LACSNP groups, corresponding to the hollow nanoparticles, which have a significant increase in ROS production also show a decrease in cell viability. Knowing this effect on ROS production, the decrease in cell viability is expected, as while ROS are essential signaling molecules involved in various cellular processes, excessive ROS production can have detrimental effects on cells. Meanwhile, in the nanoparticles

where we had the encapsulation of curcumin (CSCNP and LACSCNP), as well as for free non-encapsulated curcumin, cell viability levels were seemingly higher.

These results are aligned with the ones observed by X. Lin et al., 2019, where at higher levels of curcumin than the ones used on the present study, they could in fact see cell proliferation as well as an higher decrease in ROS production, by elevating the levels of enzymes like superoxide dismutase. This goes along with the results observed on figure 6A and 6B where on the highest concentration of free curcumin it is noticeable some degree of cell proliferation and a reduction on ROS production.

3.2.3 Nanoparticles show promising results on splenocytes

The spleen cells were incubated for 96 h with the nanoformulations, with cell viability being assessed according to the resazurin assay. To verify the effects of these curcumin loaded NPs on the inflammatory response, the capacity of production of the cytokines TNF-α and IL-6 by spleen cells was assessed after the said incubation period of 96 h with the different types of formulations. As stated before, there is a highly relevant connection between immune and inflammatory response and cancer progression, and both TNF-α and IL-6 have been the subject of several studies due to their key involvement on this intertwined dynamic.

From figure 7A, it is evident that neither of the four formulations show any kind of toxicity to splenocytes. It is even possible to observe an apparent proliferation on spleen cells in all cases, which was an effect also documented by Mustafa & Blumenthal, 2017.

Although not statistically significant, there are some variations in viability, depending on the concentration used – higher concentration of nanoparticles, which correspond to higher concentration of chitosan and curcumin, seem to have a decrease on cell viability. Even though these differences are not significant, some suppositions can be made as for the reason of this apparent decrease. Chitosan is known for being considered safe and non-toxic, however if chitosan nanoparticles are not well-dispersed or if they settle at the bottom of the culture, they may physically interfere with cell attachment, which can indirectly affect cell viability.

According to the results displayed on figure 7B and figure 7C, it appears that all the nanoparticles tested induced a small production of TNF-α. However, when looking

to the free curcumin, there doesn't seem to exist a as strong induction of this cytokine as for either curcumin-encapsulated nanoparticles or the empty ones. This suggests that the chitosan could solely be responsible for the induction of TNF-α, and the encapsulation of curcumin into these particles did not modify their ability to stimulate the secretion of TNF-α.

In fact, free curcumin shows some sort of unexpected and undocumented production of this cytokine. Curcumin has for long been described as a blocker of TNF-α production, so this could perhaps be explained through the following hypothesis. To explain it first, one must have into account that the results registered for the negative control and the effect of free curcumin on the 4 mice have very similar values in some of the individuals, with free curcumin having a considerably high SEM value. So perhaps, this could in fact not be truly a stimulus in production, but just not having any expressive effect. To clear this doubt and comprehend this it is recommended to do more trials. It's a fact that the concentration of curcumin, being 0.049 μM, could fail to provide an immune response, as it could be considered almost residual.

This conveys the idea that chitosan nanoparticles can have a pro inflammatory effects in part due to their ability to induce the production of TNF-α. This can be intertwined with the production of ROS that is displayed on figures 5B and 6B. TNF-α can stimulate the production of ROS through multiple mechanisms, such as with the upregulation of NADPH oxidase, an enzyme complex responsible for generating ROS, which will lead to its increased production. On the other hand, ROS can act as signaling molecules to activate intracellular pathways involved in the synthesis and release of TNF-α, for example, through NF-κB (Morgan et al., 2008).

The results observed regarding the production of these cytokines can be corroborated by Abdel-Hakeem et al., 2021, where breast cancer cells with an even higher concentration of curcumin and chitosan they observed no production of IL-6 nor TNF-α. *In vivo* studies with mice have also indicated that curcumin encapsulated on chitosan nanoparticles display a non-toxic profile for spleen cells while also verifying a decrease on IL-6 and TNF-α production, although higher concentrations of curcumin were used (Teng et al., 2023).

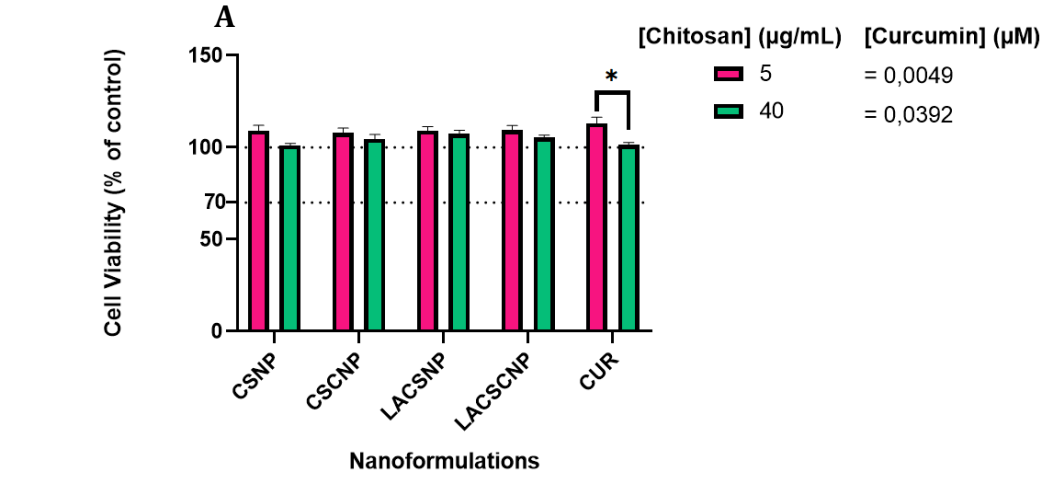

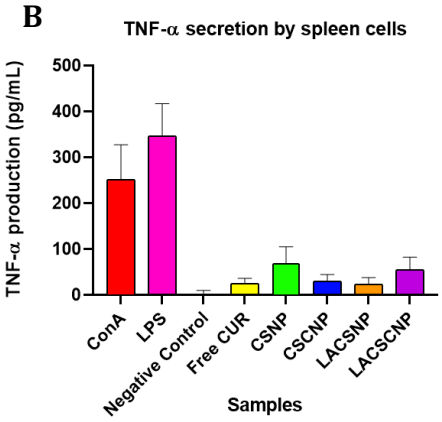

C

	TNF-α production (pg/mL) ± SEM
ConA	248.49 ±16.67
LPS	344.03 ± 45.75
Negative Control	1.54 ± 8.45
Free Curcumin	23.39 ± 12.62
CSNP	67.11 ± 37.66
CSCNP	28.35 ± 16.06
LACSNP	22.72 ± 14.82
LACSCNP	54.49 ± 27.83

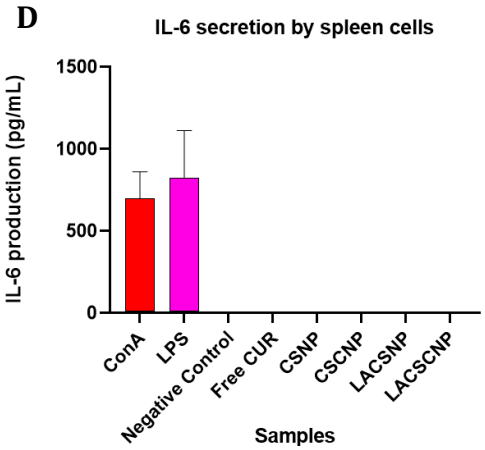

E

	IL-6 production (pg/mL) ± SEM
ConA	694.14 ± 166.17
LPS	817.67 ± 294.68
Negative Control	2.7 ± 1.56
Free Curcumin	0
CSNP	0
CSCNP	0
LACSNP	0
LACSCNP	0

Figure 7. *In vitro biological assays on spleen cells, after incubation with the different formulations for 96 h. ELISAs performed to assess cytokine production were solely conducted with the supernatants of NPs which were given 40 µg/mL of chitosan, with CSCNP and LACSCNP also having curcumin at 0.0392 µM, the same concentration as for Free CUR.* ***(A)*** *Cell viability evaluated through the resazurin assay, displayed by splenocytes, after incubation with all nanoparticles and free curcumin.* ***(B)*** *Graphic description of TNF-α concentration with different stimulus.* ***(C)*** *Quantitative description of TNF-α production with different stimulus.* ***(D)*** *Graphic description of IL-6 concentration with different stimulus.* ***(E)*** *Quantitative description of IL-6 production with different stimulus. (N=4; four independent assays, each in triplicate). Error bars represent SEM. (* = $p < 0.05$).*

3.2.4 Nanoparticles at a lower concentration show better viability on PBMCs

Following a 96 h period of incubation with the nanoformulations, cell viability was measured using the MTT assay. The results are depicted on figure 8.

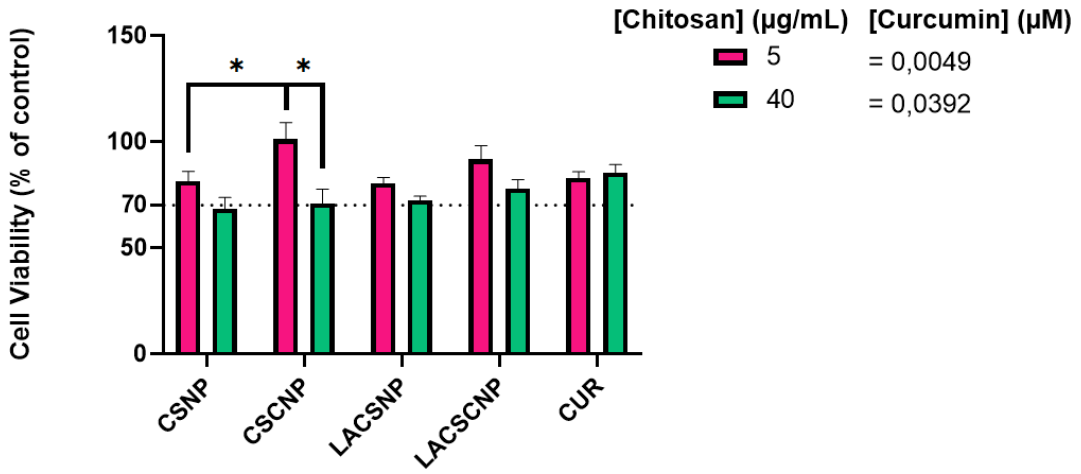

Figure 8. *Evaluation of cell viability displayed by PBMCs, after incubation with all nanoparticles and free curcumin (N=3; three independent assays, each in triplicate). Error bars represent SEM. (* = p < 0.05).*

On figure 8 we can observe that free curcumin is able to maintain cell viability values clearly above 70 %, despite of the different concentrations used. Looking at the NPs results, there is a clear decrease on cell viability when we pass from the lowest to the highest concentration.

Like the effects registered on splenocytes, higher concentrations of the nanoformulations (40 µg/mL of chitosan, corresponding to 0.0392 µM of curcumin) resulted on lower viability of PBMCS, while the lower values (5 µg/mL of chitosan, corresponding to 0.0049 µM of curcumin) had considerably good viability results. However, the results have a higher discrepancy than before, while using the same concentrations. It is worth mentioning that in Deka et al., 2016 they also verified a significant decrease on PBMCs' viability when using curcumin encapsulated with chitosan. They justify this as perhaps being due to high surface activity of the nanoparticle.

As for the difference in viability when comparing the two concentrations, this could be, again, associated to the fact that, despite not being toxic, if chitosan nanoparticles are not well-dispersed and instead settle at the bottom of the wells, they can

interfere with cell attachment, leading to and indirect impairment of cell viability by compromising the ability of cells to adhere and thrive.

From analyzing the figure 6, it is also noticeable that, for 5 μg/mL of lactobionic acid modified-chitosan particles containing 0.0049 μM of curcumin, there seems to be an increase in cell viability. This increase is visible when comparing its results to the same type of nanoparticles without curcumin, to non-modified chitosan containing curcumin and also to non-encapsulated curcumin. Having this unexpected variation could indicate a possible synergy between the modified chitosan and curcumin. In PBMCs, there are no known receptors of lactobionic acid, which is expressed on the surface of modified chitosan nanoparticles, nor any described mechanism involving the phagocytosis of lactobionic acid and cell proliferation. A possible explanation could be reliant on the alteration of the physicochemical properties of chitosan, when modified with lactobionic acid, which could, somehow, facilitate its uptake or degradation by PBMCs, thereby leading to improved values of cell viability. So, even though the only difference between the nanoparticles which obtained the highest cell viability results (LACSCNPs) and CSCNPs is the addition of lactobionic acid to chitosan's surface, there is no documented explanation for this.

3.2.5 Higher concentrations of nanoparticles lead to a small decrease in viability in neutrophils

After a 24 h period of incubation with the nanoformulations, cell viability was measured using the resazurin assay. The results are displayed on figure 9. The same observations that were previously made regarding splenocytes and PBMCs can also be done to the results extracted from the neutrophils' experiments.

Free non encapsulated curcumin seems to have higher cell viability for both concentrations, as well as also being able to reduce ROS production. There is a reduced viability when using the higher concentrations of all nanoparticles as it was already extensively described and hypothesized for both splenocytes and PBMCs.

Typically, neutrophils produce reactive oxygen species as a regular part of their immune responsibilities. Nevertheless, excessive ROS production can lead to DNA

damage, chronic inflammation, and promotion of tumor growth, which is why it is important to verify oxidative stress levels in neutrophils.

Cells were incubated with a DCFH-DA probe for 2 h, after previously being incubated for 24 h with the formulations.

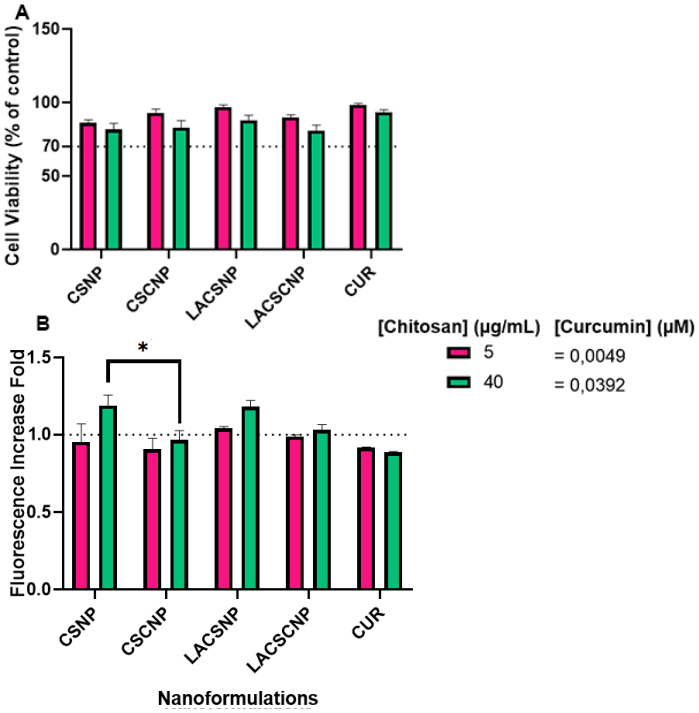

Figure 9. *Results regarding the effect of the nanoformulations on neutrophils' viability and ROS production. CSNP: Empty Chitosan Nanoparticles; CSCNP: Curcumin-Encapsulated Chitosan Nanoparticles; LACSNP: Empty Lactobionic Acid-modified Chitosan Nanoparticles; LACSCNP: Curcumin-Encapsulated Lactobionic Acid-modified Chitosan Nanoparticles; CUR: Free, non-encapsulated curcumin.* ***(A)*** *Evaluation of cell viability displayed by neutrophils, after incubation with all nanoparticles and free curcumin.* ***(B)*** *Induction of ROS production by neutrophils after 24 h of incubation with all nanoparticles and free curcumin. Error bars represent SEM. (N=3; three independent assays, each in triplicate). (* = $p < 0.05$).*

Similar to what was also verified in figure 7B and 8B, in figure 9B we can also verify the discrepancy between having hollow and curcumin-containing nanoparticles, for ROS production. The encapsulation of curcumin on both CSCNP and LACSCNP does produce a visible difference when compared to their hollow nanoparticles, with a slight decrease on ROS production. This proves that curcumin can maintain its antioxidative effect despite being encapsulated, so it means that is correctly delivered. Looking at the higher concentrations (40 µg/mL of chitosan) of CSNP and LACSNP we can see an increase in ROS production, while 5 µg/mL of chitosan in these particles does not produce any significant alteration. However, even at the

higher concentrations of chitosan, when we introduce curcumin, ROS production is significantly decreased.

By comparing both figure 9A and figure 9B, despite not existing expressively significant differences in cell viability between high and low concentrations, it is clear that higher concentrations of the nanoparticles tend to have a somewhat lower percentage of viability. This coincides with the fact that particles with 40 μg/mL of chitosan also achieve higher values of ROS production, existing a significant difference in ROS production when encapsulating curcumin.

On a similar study (Cho et al., 2020), it has also been stated that curcumin can in fact play a protective role of neutrophils, reducing TNF-α and IL-6 production when it had previously been stimulated, which is some evidence that is currently lacking on the present report. Like the results observed here, free curcumin also didn't directly affect neutrophils apoptosis. There are also studies corroborating that there is a wide range of curcumin concentrations that can reduce ROS production with also no toxicity displayed by free curcumin on neutrophils (Disbanchong et al., 2021).

Chapter 4 – Conclusions and Future Perspectives

4. Conclusions and Future Perspectives

In recent years, scientific and financial investments have been made in the areas surrounding nanotechnology, due to a high increase of interest of the industry sector on this field of study. Nonetheless, these investments are profoundly justified, as nanomedicine has continuously proved its importance on the development of more, better, and safer options regarding multiple types of preventions, diagnostics, and treatments to a wide variety of medical conditions.

The aim of this thesis, was to study chitosan and lactobionic acid-modified chitosan nanoparticles, encapsulated with curcumin. This choice was due to both curcumin and chitosan having documented beneficial effects. On one hand, curcumin is a natural polyphenol, which has been extensively studied for its potential health benefits, including anti-inflammatory, antioxidant, and anticancer properties. On the other hand, chitosan has been studied for its potential benefits such as wound healing, antimicrobial activity, and as a vehicle for targeted delivery of therapeutic agents. This last part has made chitosan gain attention in various fields, due to its biocompatibility, biodegradability, and low toxicity. These characteristics make it a perfect partner for the delivery of curcumin, which despite its helpful effects, unfortunately has poor bioavailability and is also hydrophobic, making it undergo rapid metabolism and elimination of the body, which limits its therapeutic efficacy.

The main objectives were not only to produce and characterize these said nanoparticles, but also to evaluate its cytotoxicity, influence on oxidative stress and immunomodulation on different cell types, present on the tumor microenvironment.

Empty and curcumin-containing nanoparticles were produced following the ionotropic gelation method. Its characterization and biological effects were compared throughout the works. Both types of nanoparticles were successfully produced, achieving good results overall, namely on curcumin encapsulation. The particle diameter, PDI and zeta potential were measured by DLS and ELS respectively. Dynamic light scattering (DLS) analysis confirmed the successful generation of nanoparticles with accurate and similar sizes. Furthermore, electrophoretic light scattering (ELS) provided valuable insights into the influence

of production variables on the surface charges of the nanoparticles. These surface charges play a crucial role in particle aggregation, emphasizing the need to carefully control the production parameters to optimize the nanoparticles' properties.

Concentrations to study cytotoxicity were identical for both HepG2 and Raw 264.7 cell lines as well for PBMCs, neutrophils and splenocytes with similar results: little to no toxicity in the tested concentration ranges. As for the ROS production, it was clear that while empty chitosan nanoparticles could in some cases increase this production, curcumin would stabilize it to normal values observed in the negative control or even reduce its production. From the cytokine production assay, it was verified an inability of curcumin to over impose its anti-inflammatory effects over chitosan, with a small increase in TNF-α production being of notice.

However, there are still several assays that could and should be performed in order to achieve a more profound understanding of the effect of these particles on the tumor microenvironment.

Starting with the particles themselves, it could be interesting studying the release rate of curcumin, as it could provide some more insights regarding pharmacokinetics and bioavailability of curcumin, namely, to understand if the release is controlled over time, with a constant release rate, enabling researchers to design more efficient and targeted drug delivery strategies and dosages. Cellular uptake studies could also be relevant, for the same reasons – having a better understanding of dosages, to have more optimized results.

As for the anti-cancer properties more precisely, bearing in mind the metastatic profile of hepatocellular carcinoma, it could be of use performing migration assays. The use of *in vitro* 3D tumor models, such as spheroids, could also provide a more representative environment to study the effects of the nanoparticles on a more realistic scenario.

Regarding the inflammatory response, there is still a lot to be understood, namely the production of cytokines by other types of cells, such as macrophages and neutrophils, as well as RANTES quantification assays which needs to be performed in HepG2 cells. These protocols can and should be even more optimized and

additional chitosan and curcumin concentrations need to be tested, to provide more information on the true effects of these nanoparticles.

To end my analysis, this work sat a few initial stones regarding the relation of these nano formulations with the tumor microenvironment, as well as giving some insights to its usage regarding the treatment of hepatocellular carcinoma. Nevertheless, there is still work left unfinished as I stated earlier and there is still more knowledge to be acquired regarding the interaction of these nanoparticles with the different cell lines before following the natural progression of this study which would be *in vivo* studies.

Chapter 5 - Bibliography

5. Bibliography

Abd El-Hack, M. E., El-Saadony, M. T., Shafi, M. E., Zabermawi, N. M., Arif, M., Batiha, G. E., Khafaga, A. F., Abd El-Hakim, Y. M., & Al-Sagheer, A. A. (2020). Antimicrobial and antioxidant properties of chitosan and its derivatives and their applications: A review. *International Journal of Biological Macromolecules*, *164*, 2726–2744. https://doi.org/10.1016/J.IJBIOMAC.2020.08.153

Abdel-Hakeem, M. A., Mongy, S., Hassan, B., Tantawi, O. I., & Badawy, I. (2021). Curcumin Loaded Chitosan-Protamine Nanoparticles Revealed Antitumor Activity Via Suppression of NF-κB, Proinflammatory Cytokines and Bcl-2 Gene Expression in the Breast Cancer Cells. *Journal of Pharmaceutical Sciences*, *110*(9), 3298–3305. https://doi.org/10.1016/J.XPHS.2021.06.004

Ahmad, M., Taweel, G. M. A., & Hidayathulla, S. (2018). Nano-composites chitosan-curcumin synergistically inhibits the oxidative stress induced by toxic metal cadmium. *International Journal of Biological Macromolecules*, *108*, 591–597. https://doi.org/10.1016/J.IJBIOMAC.2017.12.054

Alonso, S. (2018). Exploiting the bioengineering versatility of lactobionic acid in targeted nanosystems and biomaterials. *Journal of Controlled Release*, *287*, 216–234. https://doi.org/10.1016/J.JCONREL.2018.08.030

Arvanitakis, K., Koletsa, T., Mitroulis, I., & Germanidis, G. (2022). Tumor-Associated Macrophages in Hepatocellular Carcinoma Pathogenesis, Prognosis and Therapy. *Cancers 2022, Vol. 14, Page 226*, *14*(1), 226. https://doi.org/10.3390/CANCERS14010226

Arya, G., Das, M., & Sahoo, S. K. (2018). Evaluation of curcumin loaded chitosan/PEG blended PLGA nanoparticles for effective treatment of pancreatic cancer. *Biomedicine & Pharmacotherapy = Biomedecine & Pharmacotherapie*, *102*, 555–566. https://doi.org/10.1016/J.BIOPHA.2018.03.101

Ashtari, S., Pourhoseingholi, M. A., Sharifian, A., & Zali, M. R. (2015). Hepatocellular carcinoma in Asia: Prevention strategy and planning. *World Journal of Hepatology*, *7*(12), 1708. https://doi.org/10.4254/WJH.V7.I12.1708

Bahadur K.C., R., Lee, S. M., Yoo, E. S., Choi, J. H., & Ghim, H. Do. (2009). Glycoconjugated chitosan stabilized iron oxide nanoparticles as a multifunctional nanoprobe. *Materials Science and Engineering: C*, *29*(5), 1668–1673. https://doi.org/10.1016/J.MSEC.2009.01.005

Baldo, B. A. (2013). Adverse events to monoclonal antibodies used for cancer therapy: Focus on hypersensitivity responses. *Oncoimmunology*, *2*(10). https://doi.org/10.4161/ONCI.26333

Barry, A. E., Baldeosingh, R., Lamm, R., Patel, K., Zhang, K., Dominguez, D. A., Kirton, K. J., Shah, A. P., & Dang, H. (2020). Hepatic Stellate Cells and Hepatocarcinogenesis. *Frontiers in Cell and Developmental Biology*, *8*, 709. https://doi.org/10.3389/FCELL.2020.00709/BIBTEX

Binion, D. G., Otterson, M. F., & Rafiee, P. (2008). Curcumin inhibits VEGF-mediated angiogenesis in human intestinal microvascular endothelial cells through COX-2 and MAPK inhibition. *Gut*, *57*(11), 1509–1517. https://doi.org/10.1136/GUT.2008.152496

Camacho-Barquero, L., Villegas, I., Sánchez-Calvo, J. M., Talero, E., Sánchez-Fidalgo, S., Motilva, V., & Alarcón de la Lastra, C. (2007). Curcumin, a Curcuma longa constituent, acts on MAPK p38 pathway modulating COX-2 and iNOS expression in chronic experimental colitis. *International Immunopharmacology*, *7*(3), 333–342. https://doi.org/10.1016/J.INTIMP.2006.11.006

Cas, M. D., & Ghidoni, R. (2019). Dietary Curcumin: Correlation between Bioavailability and Health Potential. *Nutrients*, *11*(9). https://doi.org/10.3390/NU11092147

Castañeda, A. M., Meléndez, C. M., Uribe, D., & Pedroza-Díaz, J. (2022). Synergistic effects of natural compounds and conventional chemotherapeutic agents: recent insights for the development of cancer treatment strategies. *Heliyon*, *8*(6), e09519. https://doi.org/10.1016/J.HELIYON.2022.E09519

Chainani-Wu, N. (2004). Safety and Anti-Inflammatory Activity of Curcumin: A Component of Tumeric (Curcuma longa). *Https://Home.Liebertpub.Com/Acm*, *9*(1), 161–168. https://doi.org/10.1089/107555303321223035

chen, J., Yang, J., Ma, L., Li, J., Shahzad, nasir, & Kyung Kim, chan. (2020). Structure-antioxidant activity relationship of methoxy, phenolic hydroxyl, and carboxylic acid groups of phenolic acids. *Scientific RepoRtS |*, *10*, 2611. https://doi.org/10.1038/s41598-020-59451-z

Chen, L., Wang, S., Wang, Y., Zhang, W., Ma, K., Hu, C., Zhu, H., Liang, S., Liu, M., & Xu, N. (2018). IL-6 influences the polarization of macrophages and the formation and growth of colorectal tumor. *Oncotarget*, *9*(25), 17443. https://doi.org/10.18632/ONCOTARGET.24734

Chen, Z., Xie, H., Hu, M., Huang, T., Hu, Y., Sang, N., & Zhao, Y. (2020). Recent progress in treatment of hepatocellular carcinoma. *American Journal of Cancer Research*, *10*(9), 2993. /pmc/articles/PMC7539784/

Cho, K. B., Park, C. H., Kim, J., Tin, T. D., & Kwak, S.-H. (2020). Protective role of curcumin against lipopolysaccharide-induced inflammation and apoptosis in human neutrophil. *Anesthesia and Pain Medicine*, *15*(1), 41–48. https://doi.org/10.17085/APM.2020.15.1.41

Cortez-Retamozo, V., Etzrodt, M., Newton, A., Rauch, P. J., Chudnovskiy, A., Berger, C., Ryan, R. J. H., Iwamoto, Y., Marinelli, B., Gorbatov, R., Forghani, R., Novobrantseva, T. I., Koteliansky, V., Figueiredo, J. L., Chen, J. W., Anderson, D. G., Nahrendorf, M., Swirski, F. K., Weissleder, R., & Pittet, M. J. (2012). Origins of tumor-associated macrophages and neutrophils. *Proceedings of the National Academy of Sciences of the United States of America*, *109*(7), 2491–2496. https://doi.org/10.1073/PNAS.1113744109/-/DCSUPPLEMENTAL

Coussens, L. M., Zitvogel, L., & Palucka, A. K. (2013). Neutralizing Tumor-Promoting Chronic Inflammation: A Magic Bullet? *Science*, *339*(6117), 286–291.

https://doi.org/10.1126/SCIENCE.1232227

Crissien, A. M., & Frenette, C. (2014). Current Management of Hepatocellular Carcinoma. *Gastroenterology & Hepatology*, *10*.

D'Souza, A. A., & Devarajan, P. V. (2015). Asialoglycoprotein receptor mediated hepatocyte targeting - Strategies and applications. *Journal of Controlled Release*, *203*, 126–139. https://doi.org/10.1016/J.JCONREL.2015.02.022

da Fonseca, L. G., Reig, M., & Bruix, J. (2020). Tyrosine Kinase Inhibitors and Hepatocellular Carcinoma. *Clinics in Liver Disease*, *24*(4), 719–737. https://doi.org/10.1016/J.CLD.2020.07.012

Deka, C., Aidew, L., Devi, N., Buragohain, A. K., & Kakati, D. K. (2016). Synthesis of curcumin-loaded chitosan phosphate nanoparticle and study of its cytotoxicity and antimicrobial activity. *Https://Doi.Org/10.1080/09205063.2016.1226051*, *27*(16), 1659–1673. https://doi.org/10.1080/09205063.2016.1226051

Deng, G. L., Zeng, S., & Shen, H. (2015). Chemotherapy and target therapy for hepatocellular carcinoma: New advances and challenges. *World Journal of Hepatology*, *7*(5), 787. https://doi.org/10.4254/WJH.V7.I5.787

Dhar, D., Antonucci, L., Nakagawa, H., Kim, J. Y., Glitzner, E., Caruso, S., Shalapour, S., Yang, L., Valasek, M. A., Lee, S., Minnich, K., Seki, E., Tuckermann, J., Sibilia, M., Zucman-Rossi, J., & Karin, M. (2018). Liver Cancer Initiation Requires p53 Inhibition by CD44-Enhanced Growth Factor Signaling HHS Public Access. *Cancer Cell*, *33*(6), 1061–1077. https://doi.org/10.1016/j.ccell.2018.05.003

Disbanchong, P., Punmanee, W., Srithanasuwan, A., Pangprasit, N., Wongsawan, K., Suriyasathaporn, W., & Chuammitri, P. (2021). Immunomodulatory Effects of Herbal Compounds Quercetin and Curcumin on Cellular and Molecular Functions of Bovine-Milk-Isolated Neutrophils toward Streptococcus agalactiae Infection. *Animals : An Open Access Journal from MDPI*, *11*(11). https://doi.org/10.3390/ANI11113286

Etemadi, S., Barhaghi, M. H. S., Leylabadlo, H. E., Memar, M. Y., Mohammadi, A. B., & Ghotaslou, R. (2021). The synergistic effect of turmeric aqueous extract and chitosan against multidrug-resistant bacteria. *New Microbes and New Infections*, *41*. https://doi.org/10.1016/J.NMNI.2021.100861

Fridlender, Z. G., Sun, J., Kim, S., Kapoor, V., Cheng, G., Ling, L., Worthen, G. S., & Albelda, S. M. (2009). Polarization of Tumor-Associated Neutrophil (TAN) Phenotype by TGF-β: "N1" versus "N2" TAN. *Cancer Cell*, *16*(3), 183. https://doi.org/10.1016/J.CCR.2009.06.017

Garg, U., Chauhan, S., Nagaich, U., & Jain, N. (2019). Current Advances in Chitosan Nanoparticles Based Drug Delivery and Targeting. *Advanced Pharmaceutical Bulletin*, *9*(2), 195. https://doi.org/10.15171/APB.2019.023

Guo, K., Liu, Y., Zhou, H., Dai, Z., Zhang, J., Sun, R., Chen, J., Sun, Q., Lu, W., Kang, X., & Chen, P. (2008). Involvement of protein kinase C β-extracellular signal-regulating kinase1/2/p38 mitogen-activated protein kinase-heat shock protein 27 activation

in hepatocellular carcinoma cell motility and invasion. *Cancer Science*, *99*(3), 486–496. https://doi.org/10.1111/J.1349-7006.2007.00702.X

Guo, Y.-J., Pan, W.-W., Liu, S.-B., Shen, Z.-F., Xu, Y., & Hu, L.-L. (2020). ERK/MAPK signalling pathway and tumorigenesis. *Experimental and Therapeutic Medicine*, *19*(3), 1997. https://doi.org/10.3892/ETM.2020.8454

Hasegawa, M., Yagi, K., Iwakawa, S., & Hirai, M. (2001). Chitosan induces apoptosis via caspase-3 activation in bladder tumor cells. *Japanese Journal of Cancer Research*, *92*(4), 459–466. https://doi.org/10.1111/J.1349-7006.2001.TB01116.X

Hefnawy, A., Khalil, I. H., Arafa, K., Emara, M., & El-Sherbiny, I. M. (2020). Dual-Ligand Functionalized Core-Shell Chitosan-Based Nanocarrier for Hepatocellular Carcinoma-Targeted Drug Delivery. *International Journal of Nanomedicine*, *15*, 821. https://doi.org/10.2147/IJN.S240359

Holczbauer, Á., Wangensteen, K. J., & Shin, S. (2022). Cellular origins of regenerating liver and hepatocellular carcinoma. *JHEP Reports*, *4*(4). https://doi.org/10.1016/J.JHEPR.2021.100416

Hu, Q., & Luo, Y. (2021). Chitosan-based nanocarriers for encapsulation and delivery of curcumin: A review. *International Journal of Biological Macromolecules*, *179*, 125–135. https://doi.org/10.1016/J.IJBIOMAC.2021.02.216

Hu, S., Maiti, P., Ma, Q., Zuo, X., Jones, M. R., Cole, G. M., & Frautschy, S. A. (2015). Clinical development of curcumin in neurodegenerative disease. *Expert Review of Neurotherapeutics*, *15*(6), 629. https://doi.org/10.1586/14737175.2015.1044981

Huang, Q., Li, J., Zheng, J., & Wei, A. (2019). The Carcinogenic Role of the Notch Signaling Pathway in the Development of Hepatocellular Carcinoma. *Journal of Cancer*, *10*. https://doi.org/10.7150/jca.26847

Huynh, H., Wei Jie Ong, R., Yi Qing Li, P., Shean Lee, S., Yang, S., Wen Chong, L., Anh Tuan Luu, D., Tzen Jong, C., & Wei Ling Lam, I. (2012). Targeting Receptor Tyrosine Kinase Pathways in Hepatocellular Carcinoma. *Anti-Cancer Agents in Medicinal Chemistry*, *11*(6), 560–575. https://doi.org/10.2174/187152011796011055

International Organization for Standardization. (2017). ISO 22412:2017 - Particle size analysis — Dynamic light scattering (DLS). Retrieved from https://www.iso.org/obp/ui/#iso:std:iso:22412:ed-2:v1:en

Jayasingam, S. D., Citartan, M., Thang, T. H., Mat Zin, A. A., Ang, K. C., & Ch'ng, E. S. (2019). Evaluating the Polarization of Tumor-Associated Macrophages Into M1 and M2 Phenotypes in Human Cancer Tissue: Technicalities and Challenges in Routine Clinical Practice. *Frontiers in Oncology*, *9*. https://doi.org/10.3389/FONC.2019.01512

Jesus, S., Marques, A. P., Duarte, A., Soares, E., Costa, J. P., Colaço, M., … Borges, O. (2020). Chitosan Nanoparticles: Shedding Light on Immunotoxicity and Hemocompatibility. Frontiers in Bioengineering and Biotechnology, 8. https://doi.org/10.3389/FBIOE.2020.00100

Jhaveri, J., Raichura, Z., Khan, T., Momin, M., & Omri, A. (2021). Chitosan

Nanoparticles-Insight into Properties, Functionalization and Applications in Drug Delivery and Theranostics. *Molecules (Basel, Switzerland)*, *26*(2). https://doi.org/10.3390/MOLECULES26020272

Jiang, W., Li, Y., Zhang, S., Kong, G., & Li, Z. (2021). Association between cellular immune response and spleen weight in mice with hepatocellular carcinoma. *Oncology Letters*, *22*(2). https://doi.org/10.3892/OL.2021.12886

Jin, X., Zhang, S., Wang, N., Guan, L., Shao, C., Lin, Y., Liu, J., & Li, Y. (2022). High Expression of TGF-β1 Contributes to Hepatocellular Carcinoma Prognosis via Regulating Tumor Immunity. *Frontiers in Oncology*, *12*, 1598. https://doi.org/10.3389/FONC.2022.861601/BIBTEX

Karthikeyan, A., Senthil, N., & Min, T. (2020). Nanocurcumin: A Promising Candidate for Therapeutic Applications. *Frontiers in Pharmacology*, *11*, 487. https://doi.org/10.3389/FPHAR.2020.00487/BIBTEX

Khalaf, A. M., Fuentes, D., Morshid, A. I., Burke, M. R., Kaseb, A. O., Hassan, M., Hazle, J. D., & Elsayes, K. M. (2018). Role of Wnt/β-catenin signaling in hepatocellular carcinoma, pathogenesis, and clinical significance. *Journal of Hepatocellular Carcinoma*, *5*, 61–73. https://doi.org/10.2147/JHC.S156701

Khan, M. A., Zafaryab, M., Mehdi, S. H., Ahmad, I., & Rizvi, M. M. A. (2016). Characterization and anti-proliferative activity of curcumin loaded chitosan nanoparticles in cervical cancer. *International Journal of Biological Macromolecules*, *93*(Pt A), 242–253. https://doi.org/10.1016/J.IJBIOMAC.2016.08.050

Kim, G.-Y., Kim, K.-H., Lee, † Soong-Hwan, Yoon, M.-S., Lee, H.-J., Moon, D.-O., Lee, C.-M., Ahn, S.-C., Park, Y. C., & Park, Y.-M. (2005). Curcumin Inhibits Immunostimulatory Function of Dendritic Cells: MAPKs and Translocation of NF-κB as Potential Targets. *The Journal of Immunology*, *174*(12), 8116–8124. https://doi.org/10.4049/JIMMUNOL.174.12.8116

Kim, H. Y., Park, E. J., Joe, E., & Jou, I. (2003). Curcumin suppresses Janus kinase-STAT inflammatory signaling through activation of Src homology 2 domain-containing tyrosine phosphatase 2 in brain microglia. *Journal of Immunology (Baltimore, Md. : 1950)*, *171*(11), 6072–6079. https://doi.org/10.4049/JIMMUNOL.171.11.6072

Kim, S., & Abou-Alfa, G. K. (2014). The Role of Tyrosine Kinase Inhibitors in Hepatocellular Carcinoma. *Clinical Advances in Hematology & Oncology*, *12*(1).

Kleiveland, C., (2015). Peripheral Blood Mononuclear Cells. *The Impact of Food Bioactives on Health: In Vitro and Ex Vivo Models*, 161–167. https://doi.org/10.1007/978-3-319-16104-4_15

Kocaadam, ul. (2017). Curcumin, an active component of turmeric (Curcumaï¿¿longa), and its effects on health. *Critical Reviews in Food Science and Nutrition*, *57*(13), 2889–2895. https://doi.org/10.1080/10408398.2015.1077195

Lebre, F., Lavelle, E. C., & Borges, O. (2019). Easy and effective method to generate

endotoxin-free chitosan particles for immunotoxicology and immunopharmacology studies. *The Journal of Pharmacy and Pharmacology*, *71*(6), 920–928. https://doi.org/10.1111/JPHP.13082

Li, B., Shao, H., Gao, L., Li, H., Sheng, H., & Zhu, L. (2022). Nano-drug co-delivery system of natural active ingredients and chemotherapy drugs for cancer treatment: a review. *Https://Doi.Org/10.1080/10717544.2022.2094498*, *29*(1), 2130–2161. https://doi.org/10.1080/10717544.2022.2094498

Li, H., Shi, B., Yan, S., Zhao, T., Li, J., & Guo, X. (2014). Effects of Chitosan on the Secretion of Cytokines and Expression of Inducible Nitric Oxide Synthase mRNA in Peritoneal Macrophages of Broiler Chicken. *Brazilian Archives of Biology and Technology*, *57*(4), 466–471. https://doi.org/10.1590/S1516-8913201401903

Lin, W. J., & Chen, M. H. (2007). Synthesis of multifunctional chitosan with galactose as a targeting ligand for glycoprotein receptor. *Carbohydrate Polymers*, *67*(4), 474–480. https://doi.org/10.1016/J.CARBPOL.2006.06.017

Lin, X., Bai, D., Wei, Z., Zhang, Y., Huang, Y., Deng, H., & Huang, X. (2019). *Curcumin attenuates oxidative stress in RAW264.7 cells by increasing the activity of antioxidant enzymes and activating the Nrf2-Keap1 pathway*. https://doi.org/10.1371/journal.pone.0216711

Lopes, V. F., Giongo, C. N., de Almeida Campos, L., Abraham, W.-R., Mainardes, R. M., & Khalil, N. M. (2021). Chitosan Nanoparticles Potentiate the in vitro and in vivo Effects of Curcumin and other Natural Compounds. *Current Medicinal Chemistry*, *28*(24), 4935–4953. https://doi.org/10.2174/0929867328666201124152945

Madrigal-Santillán, E., Madrigal-Bujaidar, E., Álvarez-González, I., Sumaya-Martínez, M. T., Gutiérrez-Salinas, J., Bautista, M., Morales-González, Á., García-Luna Y González-Rubio, M., Aguilar-Faisal, J. L., & Morales-González, J. A. (2014). Review of natural products with hepatoprotective effects. *World Journal of Gastroenterology : WJG*, *20*(40), 14787. https://doi.org/10.3748/WJG.V20.I40.14787

Magnussen, A., & Parsi, M. A. (2013). Aflatoxins, hepatocellular carcinoma and public health. *World J Gastroenterol*, *19*(10), 1508–1512. https://doi.org/10.3748/wjg.v19.i10.1508

Mahdy, M. A. A., Akl, M. A., & Madkour, F. A. (2022). Effect of chitosan and curcumin nanoparticles against skeletal muscle fibrosis at early regenerative stage of glycerol-injured rat muscles. *BMC Musculoskeletal Disorders 2022 23:1*, *23*(1), 1–13. https://doi.org/10.1186/S12891-022-05633-X

Mansouri, K., Rasoulpoor, S., Daneshkhah, A., Abolfathi, S., Salari, N., Mohammadi, M., Rasoulpoor, S., & Shabani, S. (n.d.). *Clinical effects of curcumin in enhancing cancer therapy: A systematic review*. https://doi.org/10.1186/s12885-020-07256-8

Mathonnet, M., Descottes, B., Valleix, D., Labrousse, F., Denizot, Y., & Com, W. (2006). VEGF in hepatocellular carcinoma and surrounding cirrhotic liver tissues. *World J Gastroenterol*, *12*(5), 830–831. www.wjgnet.com

Mazzarino, L., Loch-Neckel, G., Dos Santos Bubniak, L., Mazzucco, S., Santos-Silva, M. C., Borsali, R., & Lemos-Senna, E. (2015). Curcumin-Loaded Chitosan-Coated Nanoparticles as a New Approach for the Local Treatment of Oral Cavity Cancer. *Journal of Nanoscience and Nanotechnology*, *15*(1), 781–791. https://doi.org/10.1166/JNN.2015.9189

Mo, E., Ebedy, Y. A., Ibrahim, M. A., Farroh, K. Y., & Hassanen, E. I. (123 C.E.). *Newly synthesized chitosan-nanoparticles attenuate carbendazim hepatorenal toxicity in rats via activation of Nrf2/HO1 signalling pathway*. https://doi.org/10.1038/s41598-022-13960-1

Mohamed Zedan, A., Fathalla Dawoud, S., & Mostafa Al-Akra, T. (2021). Hepatoprotective Effects of Chitosan and Chitosan Nanoparticles against Biochemical, Genetic, and Histological Disorders Induced by the Toxicity of Emamectin Benzoate. *Reports of Biochemistry & Molecular Biology*, *10*(3). www.RBMB.net

Mohyuddin, S. G., Qamar, A., Hu, C. ying, Chen, S. W., Wen, J. ying, Liu, X. xi, Ma, X. bin, Yu, Z. chao, Yong, Y. hong, Wu, L. Y., Bao, M. L., & Ju, X. H. (2021). Effect of chitosan on blood profile, inflammatory cytokines by activating TLR4/NF-κB signaling pathway in intestine of heat stressed mice. *Scientific Reports 2021 11:1*, *11*(1), 1–13. https://doi.org/10.1038/s41598-021-98931-8

Morgan, M. J., Kim, Y. S., & Liu, Z. G. (2008). TNFalpha and reactive oxygen species in necrotic cell death. *Cell Research*, *18*(3), 343–349. https://doi.org/10.1038/CR.2008.31

Morris, G. A., Castile, J., Smith, A., Adams, G. G., & Harding, S. E. (2011). The effect of prolonged storage at different temperatures on the particle size distribution of tripolyphosphate (TPP) – chitosan nanoparticles. *Carbohydrate Polymers*, *84*(4), 1430–1434. https://doi.org/10.1016/J.CARBPOL.2011.01.044

Mustafa, R., & Blumenthal, E. (2017). Immunomodulatory effects of turmeric: Proliferation of spleen cells in mice. *Journal of Immunoassay & Immunochemistry*, *38*(2), 140–146. https://doi.org/10.1080/15321819.2016.1227835

Nguyen-Lefebvre, A. T., & Horuzsko, A. (2015). Kupffer Cell Metabolism and Function. Journal of Enzymology and Metabolism, 1(1). Retrieved from /pmc/articles/PMC4771376/

Nisar, S., Masoodi, T., Prabhu, K. S., Kuttikrishnan, S., Zarif, L., Khatoon, S., Ali, S., Uddin, S., Akil, A. A. S., Singh, M., Macha, M. A., & Bhat, A. A. (2022). Natural products as chemo-radiation therapy sensitizers in cancers. *Biomedicine & Pharmacotherapy*, *154*, 113610. https://doi.org/10.1016/J.BIOPHA.2022.113610

Nisari, M., Yılmaz, S., Ertekin, T., Ceylan, D., İnanç, N., Al, Ö., & Ülger, H. (2017). Effects of Curcumin on Lipid Peroxidation and Antioxidant Enzymes in Kidney, Liver, Brain and Testis of Mice Bearing Ehrlich Solid Tumor. *Proceedings 2017, Vol. 1, Page 994*, *1*(10), 994. https://doi.org/10.3390/PROCEEDINGS1100994

Omer, R. E., Bakker, M. I., Van't Veer, P., Hoogenboom, R. L. A. P., Polman, T. H. G., Alink, G. M., Idris, M. O., Kadaru, A. M. Y., & Kok, F. J. (1998). Aflatoxin and liver

cancer in sudan. *Nutrition and Cancer*, *32*(3), 174–180. https://doi.org/10.1080/01635589809514737

Pang, Y., Eresen, A., Zhang, Z., Hou, Q., Wang, Y., Yaghmai, V., & Zhang, Z. (2022). Adverse events of sorafenib in hepatocellular carcinoma treatment. *Am J Cancer Res*, *12*(6), 2770–2782. www.ajcr.us/

Peng, W.-T., Sun, W.-Y., Li, X.-R., Sun, J.-C., Du, J.-J., & Wei, W. (n.d.). *Molecular Sciences Emerging Roles of G Protein-Coupled Receptors in Hepatocellular Carcinoma*. https://doi.org/10.3390/ijms19051366

Petrick, J. L., Campbell, P. T., Koshiol, J., Thistle, J. E., Andreotti, G., Beane-Freeman, L. E., Buring, J. E., Chan, A. T., Chong, D. Q., Doody, M. M., Gapstur, S. M., Gaziano, J. M., Giovannucci, E., Graubard, B. I., Lee, I.-M., Liao, L. M., Linet, M. S., Palmer, J. R., Poynter, J. N., … Mcglynn, K. A. (2018). *ARTICLE Epidemiology Tobacco, alcohol use and risk of hepatocellular carcinoma and intrahepatic cholangiocarcinoma: The Liver Cancer Pooling Project*. https://doi.org/10.1038/s41416-018-0007-z

Pokhrel, S., & Yadav, P. N. (2019). Functionalization of chitosan polymer and their applications. *Journal of Macromolecular Science, Part A: Pure and Applied Chemistry*, *56*(5), 450–475. https://doi.org/10.1080/10601325.2019.1581576/FORMAT/EPUB

Psilopatis, I., Damaskos, C., Garmpi, A., Sarantis, P., Koustas, E., Antoniou, E. A., Dimitroulis, D., Kouraklis, G., Karamouzis, M. V., Vrettou, K., Marinos, G., Kontzoglou, K., & Garmpis, N. (2023). FDA-Approved Monoclonal Antibodies for Unresectable Hepatocellular Carcinoma: What Do We Know So Far? *International Journal of Molecular Sciences*, *24*(3). https://doi.org/10.3390/IJMS24032685

Puluhulawa, L. E., Joni, I. M., Elamin, K. M., Mohammed, A. F. A., Muchtaridi, M., & Wathoni, N. (2022). Chitosan–Hyaluronic Acid Nanoparticles for Active Targeting in Cancer Therapy. *Polymers*, *14*(16). https://doi.org/10.3390/POLYM14163410

Roggenbuck, D., Mytilinaiou, M. G., Sergey, •, Lapin, V., Reinhold, D., & Conrad, K. (n.d.). *Asialoglycoprotein receptor (ASGPR): a peculiar target of liver-specific autoimmunity*. https://doi.org/10.1007/s13317-012-0041-4

Saheb, M., Fereydouni, N., Nemati, S., Barreto, G. E., Johnston, T. P., & Sahebkar, A. (2019). Chitosan-based delivery systems for curcumin: A review of pharmacodynamic and pharmacokinetic aspects. *Journal of Cellular Physiology*, *234*(8), 12325–12340. https://doi.org/10.1002/JCP.28024

Sevic, I., Spinelli, F. M., Cantero, M. J., Reszegi, A., Kovalszky, I., García, M. G., & Alaniz, L. (2019). The Role of the Tumor Microenvironment in the Development and Progression of Hepatocellular Carcinoma. *Hepatocellular Carcinoma*, 29–45. https://doi.org/10.15586/HEPATOCELLULARCARCINOMA.2019.CH2

Sharan Adhikari, H., & Nath Yadav, P. (2018). *Anticancer Activity of Chitosan, Chitosan Derivatives, and Their Mechanism of Action*. https://doi.org/10.1155/2018/2952085

Shi, B., Abrams, M., & Sepp-Lorenzino, L. (2013). Expression of Asialoglycoprotein

Receptor 1 in Human Hepatocellular Carcinoma. *Journal of Histochemistry and Cytochemistry*, *61*(12), 901. https://doi.org/10.1369/0022155413503662

Siracusano, G., Tagliamonte, M., Buonaguro, L., & Lopalco, L. (n.d.). *Cell Surface Proteins in Hepatocellular Carcinoma: From Bench to Bedside*. https://doi.org/10.3390/vaccines8010041

Sun, E. J., Wankell, M., Palamuthusingam, P., McFarlane, C., & Hebbard, L. (2021). Targeting the PI3K/Akt/mTOR Pathway in Hepatocellular Carcinoma. *Biomedicines*, *9*(11). https://doi.org/10.3390/BIOMEDICINES9111639

Szymańska, E., & Winnicka, K. (2015). Stability of chitosan - A challenge for pharmaceutical and biomedical applications. *Marine Drugs*, *13*(4), 1819–1846. https://doi.org/10.3390/MD13041819

Tan, W., Luo, X., Li, W., Zhong, J., Cao, J., Zhu, S., Chen, X., Zhou, R., Shang, C., & Chen, Y. (2019). TNF-α is a potential therapeutic target to overcome sorafenib resistance in hepatocellular carcinoma. *EBioMedicine*, *40*, 446. https://doi.org/10.1016/J.EBIOM.2018.12.047

Tanabe, T., Pricer, W. E., & Ashwell, G. (1979). Subcellular membrane topology and turnover of a rat hepatic binding protein specific for asialoglycoproteins. *Journal of Biological Chemistry*, *254*(4), 1038–1043. https://doi.org/10.1016/S0021-9258(17)34164-9

Teng, L., Zhang, Y., Chen, L., & Shi, G. (2023). Fabrication of a curcumin encapsulated bioengineered nano-cocktail formulation for stimuli-responsive targeted therapeutic delivery to enhance anti-inflammatory, anti-oxidant, and anti-bacterial properties in sepsis management. *Journal of Biomaterials Science. Polymer Edition*. https://doi.org/10.1080/09205063.2023.2181554

Tsoulfas, G., Agorastou, P., Tooulias, A., & Marakis, G. N. (2014). Current and Future Challenges in the Surgical Treatment of Hepatocellular Carcinoma: A Review. *Int Surg*, *99*, 779–786. https://doi.org/10.9738/INTSURG-D-13-00122.1

Tummala, K. S., Brandt, M., Teijeiro, A., Graña, O., Schwabe, R. F., Perna, C., & Djouder, N. (2017). Hepatocellular Carcinomas Originate Predominantly from Hepatocytes and Benign Lesions from Hepatic Progenitor Cells. *Cell Reports*, *19*(3), 584. https://doi.org/10.1016/J.CELREP.2017.03.059

Usman, S., Khawer, M., Rafique, S., Naz, Z., & Saleem, K. (2020). *The current status of anti-GPCR drugs against different cancers*. https://doi.org/10.1016/j.jpha.2020.01.001

Vllasaliu, D., Exposito-Harris, R., Heras, A., Casettari, L., Garnett, M., Illum, L., & Stolnik, S. (2010). Tight junction modulation by chitosan nanoparticles: Comparison with chitosan solution. *International Journal of Pharmaceutics*, *400*(1–2), 183–193. https://doi.org/10.1016/J.IJPHARM.2010.08.020

Wagle, N. S., & Spencer, J. C. (2021). Challenges for Measuring Cost-effectiveness of Immunotherapy in Unresectable Hepatocellular Carcinoma. *JAMA Network Open*, *4*(4). https://doi.org/10.1001/JAMANETWORKOPEN.2021.5476

Wang, H., Zhang, H., Wang, Y., Brown, Z. J., Xia, Y., Huang, Z., Shen, C., Hu, Z., Beane, J., Ansa-Addo, E. A., Huang, H., Tian, D., & Tsung, A. (2021). Regulatory T-cell and neutrophil extracellular trap interaction contributes to carcinogenesis in non-alcoholic steatohepatitis. *Journal of Hepatology*, *75*(6), 1271–1283. https://doi.org/10.1016/j.jhep.2021.07.032

Wang, J., Zhang, Z., Ai, Y., Liu, F., Chen, M. M., & Liu, D. (2021). Lactobionic acid-modified thymine-chitosan nanoparticles as potential carriers for methotrexate delivery. *Carbohydrate Research*, *501*. https://doi.org/10.1016/J.CARRES.2021.108275

Wang, Naizhi, Feng, T., Liu, X., & Liu, Q. (2020). Curcumin inhibits migration and invasion of non-small cell lung cancer cells through up-regulation of miR-206 and suppression of PI3K/AKT/mTOR signaling pathway. *Acta Pharmaceutica (Zagreb, Croatia)*, *70*(3), 399–409. https://doi.org/10.2478/ACPH-2020-0029

Wang, Nuozhou, Wang, S., Li, M. Y., Hu, B. G., Liu, L. P., Yang, S. L., Yang, S., Gong, Z., Lai, P. B. S., & Chen, G. G. (2018). Cancer stem cells in hepatocellular carcinoma: an overview andpromising therapeutic strategies. *Therapeutic Advances in Medical Oncology*, *10*. https://doi.org/10.1177/1758835918816287

Wen, N., Cai, Y., Li, F., Ye, H., Tang, W., Song, P., & Cheng, N. (2022). The clinical management of hepatocellular carcinoma worldwide: A concise review and comparison of current guidelines: 2022 update. *BioScience Trends*, *16*(1). https://doi.org/10.5582/bst.2022.01061

Wimardhani, Y. S., Suniarti, D. F., Freisleben, H. J., Wanandi, S. I., Siregar, N. C., & Ikeda, M. A. (2014). Chitosan exerts anticancer activity through induction of apoptosis and cell cycle arrest in oral cancer cells. *Journal of Oral Science*, *56*(2), 119–126. https://doi.org/10.2334/JOSNUSD.56.119

Xu, L., Wang, X., Liu, Y., Yang, G., Falconer, R. J., & Zhao, C.-X. (2022). Lipid Nanoparticles for Drug Delivery. *Advanced NanoBiomed Research*, *2*(2), 2100109. https://doi.org/10.1002/ANBR.202100109

Xu, M., Yang, L., Lin, Y., Lu, Y., Bi, X., Jiang, T., Deng, W., Zhang, L., Yi, W., Xie, Y., & Li, M. (2022). Emerging nanobiotechnology for precise theranostics of hepatocellular carcinoma. *Journal of Nanobiotechnology 2022 20:1*, *20*(1), 1–21. https://doi.org/10.1186/S12951-022-01615-2

Yang, J. D., Hainaut, P., Gores, G. J., Amadou, A., Plymoth, A., & Roberts, L. R. (2019). A global view of hepatocellular carcinoma: trends, risk, prevention and management HHS Public Access. *Nat Rev Gastroenterol Hepatol*, *16*(10), 589–604. https://doi.org/10.1038/s41575-019-0186-y

Yang, Q., Li, Y., Tuohuti, P., Qin, Z., Zhang, Z., Zhao, W., & Su, B. (2021). Advances in the Development of Biomaterials for Endotoxin Adsorption in Sepsis. Frontiers in Bioengineering and Biotechnology, 9, 699418. https://doi.org/10.3389/FBIOE.2021.699418/BIBTEX

Yang, Z., Qin, W., Chen, Y., Yuan, B., Song, X., Wang, B., Shen, F., Fu, J., & Wang, H. (2018). Cholesterol inhibits hepatocellular carcinoma invasion and metastasis by

promoting CD44 localization in lipid rafts. *Cancer Letters*, *429*, 66–77. https://doi.org/10.1016/J.CANLET.2018.04.038

Younossi, Z. M., Otgonsuren, M., Henry, L., Venkatesan, C., Mishra, A., Erario, M., & Hunt, S. (2015). Association of nonalcoholic fatty liver disease (NAFLD) with hepatocellular carcinoma (HCC) in the United States from 2004 to 2009. *Hepatology*, *62*(6), 1723–1730. https://doi.org/10.1002/HEP.28123

Zaharoff, D. A., Rogers, C. J., Hance, K. W., Schlom, J., & Greiner, J. W. (2007). Chitosan solution enhances both humoral and cell-mediated immune responses to subcutaneous vaccination. *Vaccine*, *25*(11), 2085. https://doi.org/10.1016/J.VACCINE.2006.11.034

Zhang, Jian, Zhu, X., Jin, Y., Shan, W., & Huang, Y. (2014). Mechanism study of cellular uptake and tight junction opening mediated by goblet cell-specific trimethyl chitosan nanoparticles. *Molecular Pharmaceutics*, *11*(5), 1520–1532. https://doi.org/10.1021/MP400685V/ASSET/IMAGES/LARGE/MP-2013-00685V_0008.JPEG

Zhang, Jun, He, X., Wan, Y., Zhang, H., Tang, T., Zhang, M., Yu, S., Zhao, W., & Chen, L. (n.d.). *CD44 promotes hepatocellular carcinoma progression via upregulation of YAP*. https://doi.org/10.1186/s40164-021-00247-w

Zhang, Q. Y., Wang, F. X., Jia, K. K., & Kong, L. D. (2018). Natural Product Interventions for Chemotherapy and Radiotherapy-Induced Side Effects. *Frontiers in Pharmacology*, *9*(NOV), 1253. https://doi.org/10.3389/FPHAR.2018.01253

Zhang, Y. H., Yan, H. Q., Wang, F., Wang, Y. Y., Jiang, Y. N., Wang, Y. N., & Gao, F. G. (2015). TIPE2 inhibits TNF-α-induced hepatocellular carcinoma cell metastasis via Erk1/2 downregulation and NF-κB activation. *International Journal of Oncology*, *46*(1), 254–264. https://doi.org/10.3892/IJO.2014.2725

Zheng, X., Jin, W., Wang, S., & Ding, H. (2021). Progression on the Roles and Mechanisms of Tumor-Infiltrating T Lymphocytes in Patients With Hepatocellular Carcinoma. *Frontiers in Immunology*, *12*(September), 1–11. https://doi.org/10.3389/fimmu.2021.729705

Zhou, F., & Sun, X. (n.d.). *Cholesterol Metabolism: A Double-Edged Sword in Hepatocellular Carcinoma*. https://doi.org/10.3389/fcell.2021.762828

Zhou, S. L., Zhou, Z. J., Hu, Z. Q., Huang, X. W., Wang, Z., Chen, E. B., Fan, J., Cao, Y., Dai, Z., & Zhou, J. (2016). Tumor-Associated Neutrophils Recruit Macrophages and T-Regulatory Cells to Promote Progression of Hepatocellular Carcinoma and Resistance to Sorafenib. *Gastroenterology*, *150*(7), 1646-1658.e17. https://doi.org/10.1053/j.gastro.2016.02.040

Zhu, Y.-J., Zheng, B., Wang, H.-Y., & Chen, L. (2017). New knowledge of the mechanisms of sorafenib resistance in liver cancer. *Nature Publishing Group*, *38*, 614–622. https://doi.org/10.1038/aps.2017.5

Chapter 6 – Supplementary Data

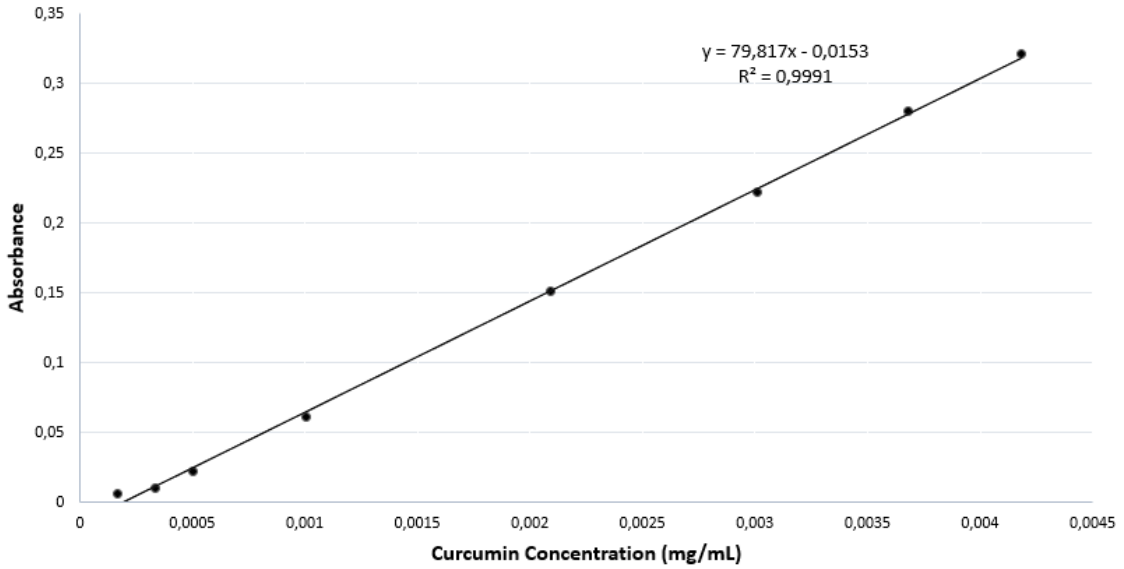

Annex 1. *Calibration curve to calculate curcumin concentration, necessary to determine NPs' encapsulation efficiency of curcumin. Reference concentrations (mg/mL) are 0.0041841, 0.003682008, 0.003012552, 0.00209205, 0.001004184, 0.000502092, 0.000334728 and 0.000167364.*

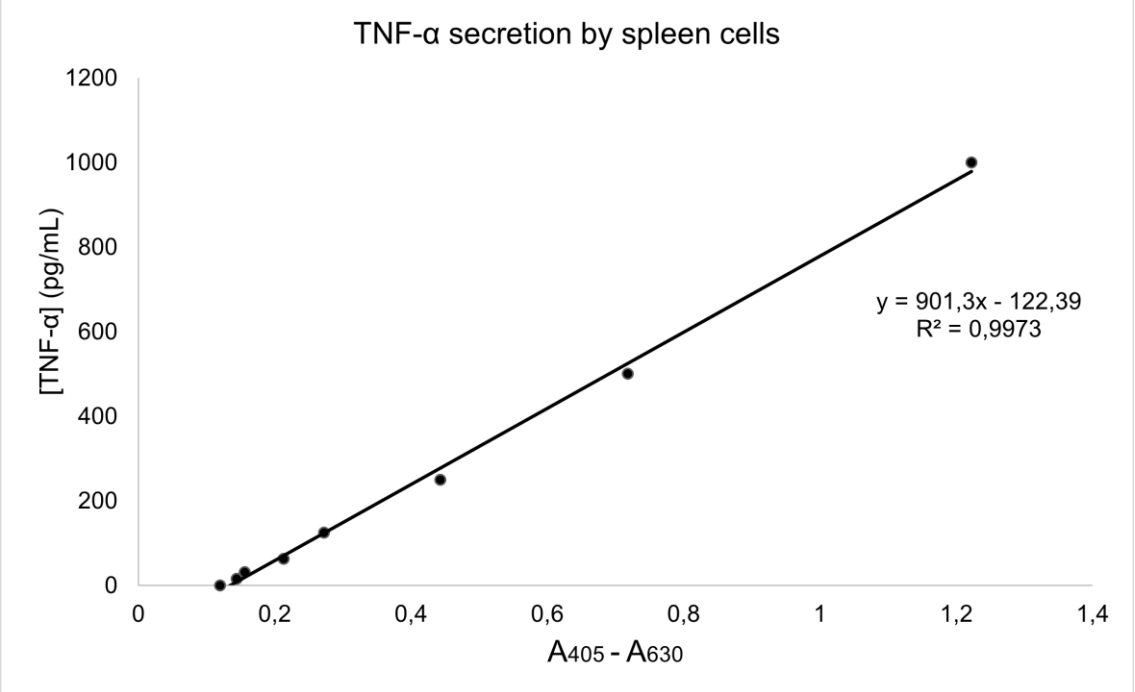

Annex 2. *Calibration curve to determine TNF-α production by spleen cells when incubated with the NPs. Reference concentrations (pg/mL) are 1000, 500, 250, 125, 62.5, 31.25, 15.625 and 0.*

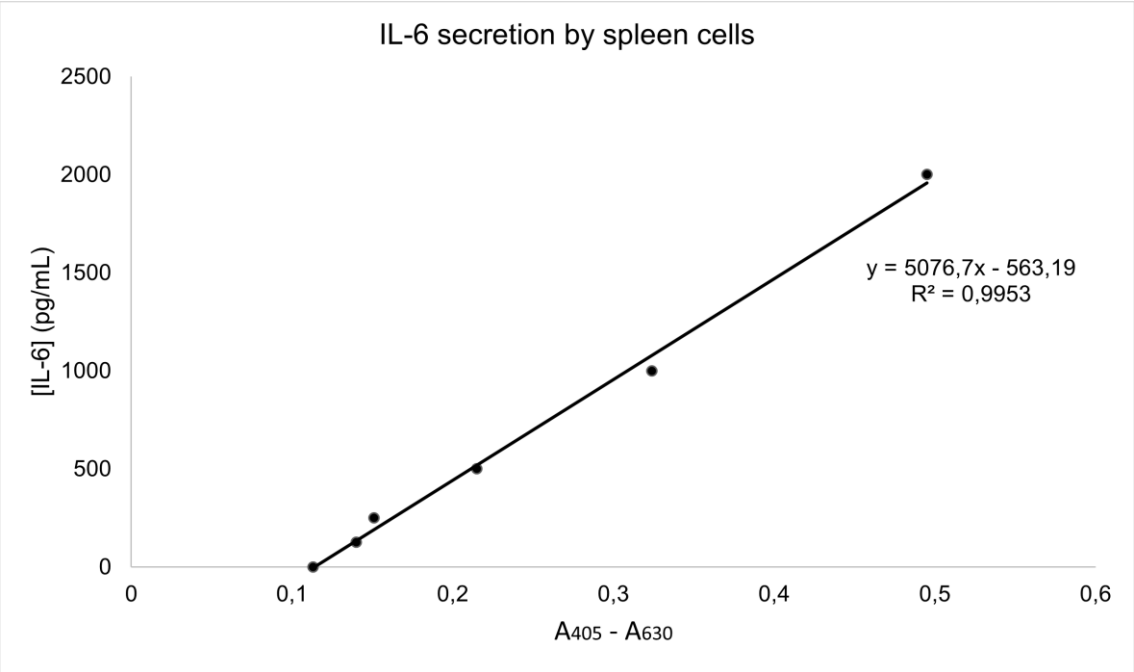

Annex 3. *Calibration curve to determine IL-6 production by spleen cells when incubated with the NPs. Reference concentrations (pg/mL) are 2000, 1000, 500, 250, 125, 62.5, 31.25 and 0.*